Published for SISSA by Springer

Received: January 11, 2014
Revised: October 8, 2014
Accepted: December 15, 2014
Published: January 12, 2015

Proton decay and new contribution to $0\nu2\beta$ decay in SO(10) with low-mass Z' boson, observable $n-\bar{n}$ oscillation, lepton flavor violation, and rare kaon decay

M.K. Parida,[a] **Ram Lal Awasthi**[b] **and P.K. Sahu**[c]

[a] *Center of Excellence in Theoretical and Mathematical Sciences, Siksha 'O' Anusandhan University, Bhubaneswar-751030, India*
[b] *Harish-Chandra Research Institute, Chhatnag Road, Jhusi, Allahabad-211019, India*
[c] *Institute of Physics, Sachivalaya Marg, Bhubaneswar, Odisha-751005, India*

E-mail: minaparida@soauniversity.ac.in, awasthi.r6@gmail.com, pradip@iopb.res.in

Abstract: In the conventional approach to observable $n-\bar{n}$ oscillation through Pati-Salam intermediate gauge symmetry in SO(10), the canonical seesaw mechanism is also constrained by the symmetry breaking scale $M_R \sim M_C \leq 10^6$ GeV which yields light neutrino masses several orders larger than the neutrino oscillation data. A method to evade this difficulty is through TeV scale gauged inverse seesaw mechanism which has been recently exploited while predicting experimentally verifiable $W_R^{\pm}, Z_R$ bosons with a new dominant contribution to neutrinoless double beta decay in the W_L-W_L channel and other observable phenomena, but with proton lifetime far beyond the accessible limits. In the present work, adopting the view that $W_R^{\pm}$ may be heavy and currently inaccessible to accelerator tests, we show how a class of non-supersymmetric SO(10) models allows a TeV scale Z' boson, experimentally testable proton decay along with observable $n-\bar{n}$ oscillation, and lepto-quark gauge boson mediated rare kaon decays without resorting to additional fine-tuning of parameters. The occurrence of Pati-Salam gauge symmetry with unbroken D-parity and two gauge couplings at the highest intermediate scale guarantees precision unification with vanishing GUT-threshold or gravitational corrections on $\sin^2\theta_W(M_Z)$ prediction in this model. Predictions for neutrinoless double beta decay in the W_L-W_L channel is analysed in detail including light and heavy sterile neutrino exchange contributions by means of normal and band plots and also by scattered plots while a new formula for half-life is derived. Comparison with available data from various groups by normal and scattered plots reveals how the existing experimental bounds are satisfied irrespective of the mass

doi:10.1007/JHEP01(2015)045

hierarchy in the light neutrino sector leading to the lower bound on the lightest sterile neutrino mass, $\hat{M}_{S_1} \geq 18 \pm 2.9\,\mathrm{GeV}$. The model also predicts branching ratios for charged lepton flavor violation verifiable by ongoing search experiments. We also derive new renormalisation group equations constraining the lepto-quark gauge boson mass in the presence of $\mathrm{SU}(2)_L \times \mathrm{U}(1)_R \times \mathrm{U}(1)_{B-L} \times \mathrm{SU}(3)_C$ symmetry, specific to the occurrence of extra Z' boson, leading to a new lower bound on the lepto-quark gauge boson mass mediating rare kaon decay, $M_{\mathrm{LQ}} \geq (1.54 \pm 0.06) \times 10^6\,\mathrm{GeV}$. We also discuss the symmetry breaking of non-SUSY SO(10) through the well known flipped $\mathrm{SU}(5) \times \tilde{\mathrm{U}}(1)$ path and show, for the first time, how TeV scale Z' is predicted with gauged inverse seesaw ansatz for neutrino masses and substantial lepton flavor and lepton number violations. As a significant new result along this path, we report a successful unification of the two gauge couplings of $\mathrm{SU}(5) \times \tilde{\mathrm{U}}(1)$ into the single GUT coupling of SO(10).

Keywords: Beyond Standard Model, GUT

ArXiv ePrint: 1401.1412v1

JHEP01(2015)045

Contents

JHEP01(2015)045

1 Introduction

Although the standard model (SM) of strong, weak, and electromagnetic interactions has unravelled the gauge origin of fundamental forces and the structure of the universe while successfully confronting numerous experimental tests, it has a number of limitations. Experimental evidences of tiny neutrino masses compared to their charged lepton counterparts also raises the fundamental issue on the origin of these masses as well as the nature of neutrinos: whether Dirac [1] or Majorana [2]- a question whose answer rests on the detection and confirmation of $0\nu\beta\beta$ decay process on which there are a number of ongoing experiments [3–11]. While direct measurement of neutrino mass by KATRIN experiment is expected to probe $m_{\nu_1} \simeq 0.2\,\text{eV}$ [12], quasi-degeneracy of neutrino masses are constrained from PLANCK satellite data on the sum of three active neutrino masses [13]. The SM predicts lepton flavor violating (LFV) decays many orders smaller than the current experimental limits which appear to be compatible via supersymmetric theories. Thus, in the absence of supersymmetry so far, it is important to explore non-supersymmetric (non-SUSY) extensions of the SM with sizeable LFV decay branching ratios.

Several limitations of the SM are removed when it is embedded in a popular grand unified theory (GUT) like SO(10) which has potentialities to achieve precision unification of the three forces, accommodate tiny neutrino masses through various seesaw mechanisms [14–20], provide spontaneous origins of Parity and CP-violations [21–25], and a host of other interesting physical phenomena. Even without any additional flavor symmetry, the model succeeds in representing all fermion masses of three generations while observable baryon number violating processes are generic among its predictions of new physics beyond the SM. Apart from proton decay, theoretical models have been proposed for experimentally observable signature of the other baryon number violating process such as $n - \bar{n}$ and $H - \bar{H}$ oscillations, and double proton decay through GUTs out of which $n - \bar{n}$ oscillation has attracted considerable interest. While in most of the conventional models [25–27, 36, 37], the intermediate breaking of Pati-Salam gauge symmetry $\text{SU}(2)_L \times \text{SU}(2)_R \times \text{SU}(4)_C (\equiv G_{224})$ has been exploited at $\mu = M_C \sim 10^6\,\text{GeV}$, in a very interesting recent development it has been proposed [29–31] to realize the process even if the symmetry breaks near the GUT scale such that the SM gauge symmetry rules all the way down to the electroweak scale. In this model the diquark Higgs mediating the oscillation process are tuned to have masses at the desired intermediate scale or lower. The model also explains the observed baryon asymmetry of the universe by a novel mechanism. Prediction of $|\Delta(B-L)| \neq 0$ proton decay mode is another special attractive feature of this model. The neutrino masses and mixings in these models are governed by high scale canonical or type-II seesaw mechanisms with $B - L$ gauge symmetry breaking occurring near the GUT-scale.

We consider worth while to pursue the conventional approach mainly because, even without resorting to additional fine tuning of parameters, we are interested in associating most of the relevant physical mass scales with the spontaneous breakings of respective intermediate gauge symmetries. A non-standard extra Z' boson which is under experimental investigation at LHC energies [32, 33] is possible by extension of the SM. If such

JHEP01(2015)045

an extension is through Pati-Salam symmetry at higher scale, the model has the interesting possibility of accommodating observable $n-\bar{n}$ oscillation and rare kaon decays. If Pati-Salam symmetry in turn emerges from a GUT scenario like SO(10), it provides interesting possibilities of gauge coupling unification and GUT-scale representation of all charged fermion masses with the prediction of Dirac neutrino mass matrix. If one fermion singlet per generation is added to the SO(10) frame work, it has the interesting possibility of explaining light neutrino masses and mixings by experimentally verifiable gauged inverse seesaw mechanism. Whereas the non-supersymmetric SM as such predicts negligible contributions to charged LFV decays, the TeV scale inverse seesaw mechanism predicts LFV branching ratios only $4-5$ order smaller than the current experimental limits. Embedding such a mechanism through heavier right-handed neutrinos provides further interesting realisation of additional new dominant contributions to neutrino-less double-beta decay in the $W_L - W_L$ channel through the exchanges of sterile neutrinos which turn out to be Majorana fermions in the model. In this work we attempt to revive the conventional approach [34–37] but by evading the light neutrino mass constraint through inverse seesaw formula gauged by the TeV scale symmetry $\mathrm{SU}(2)_L \times \mathrm{U}(1)_R \times \mathrm{U}(1)_{B-L} \times \mathrm{SU}(3)_C$ manifesting in an extra Z' boson which might be detected by ongoing search experiments at the Large Hadron Collider, a strategy which has been adopted recently in non-SUSY SO(10) GUT [39, 71]. Low energy signature of lepto-quark gauge bosons is also predicted through rare kaon decay $K_L \to \mu\bar{e}$ with branching ratios close to the current experimental limit [38]. Once the experimentally testable gauged inverse seesaw mechanism is made operative, the model is found to predict a number of new physical quantities to be verified by ongoing search experiments at low and accelerator energies. They include (i) dominant contribution to $0\nu\beta\beta$ rate in the $W_L - W_L$ channel due to heavy sterile neutrino exchanges leading to the lower bound on the lightest sterile neutrino mass $\hat{M}_{S_1} \geq 18.0 \pm 2.9\,\mathrm{GeV}$, (ii) unitarity-violating contributions to branching ratios for LFV decays, (iii) leptonic CP-violation due to non-unitarity effects, (iv) experimentally verifiable $|\Delta(B-L)| = 0$ proton decay modes such as $p \to e^+\pi^0$ (v) lepto-quark gauge-boson mediated rare kaon decay with $\mathrm{Br.}(K_L \to \mu\bar{e}) \simeq 10^{-12}$, and (vi) observable $n-\bar{n}$-oscillation mixing time $10^8 - 10^{13}$ sec with the possibility of a diquark Higgs scalar at the TeV scale.

The quark-lepton symmetric origin of the Dirac neutrino mass matrix (M_D) is found to play a crucial role in enhancing the effective mass parameter for $0\nu\beta\beta$ decay. We also briefly discuss how a constrained (unconstrained) value of the RH neutrino mass matrix emerges from the SO(10) structure with one 126 (two 126's) from the GUT-scale fit to charged fermion masses.

Although some of the results of the present work were also derived in a recent work [39], the model required the asymmetric left-right gauge symmetry at $\simeq 10\,\mathrm{TeV}$ leading to the prediction of $W_R^{\pm}, Z_R$ gauge bosons at LHC energies. In the present SO(10) model, we show that even though only a TeV scale Z' boson [42–47] is detected at the LHC, a number of these observable predictions are still applicable even if the $W_R^{\pm}$ boson masses are beyond the currently accessible LHC limit. In contrast to the earlier model, in the present work we predict proton lifetime to be accessible to ongoing search experiments. The symmetry breaking chain of the model is found to require $\mathrm{SU}(2)_L \times \mathrm{SU}(2)_R \times \mathrm{SU}(4)_C \times D(g_{2L} = g_{2R})(\equiv g_{224D})$

JHEP01(2015)045

gauge symmetry at the highest intermediate scale (M_P) which eliminates the possible presence of triangular geometry of gauge couplings around the GUT scale. This in turn determines the unification mass precisely, at the meeting point of two gauge coupling constant lines. In contrast to near Planck scale unification of ref. [39] in this work we obtain $M_U = 10^{15.95}\,\text{GeV}$ in the minimal model, but $M_U = 10^{15.5}\,\text{GeV}$ in the bi-triplet-extended non-minimal model. The other advantage of this symmetry is that it pushes most of the larger-sized submultiplets down to the parity restoring intermediate scale reducing the size of GUT-threshold effects on the unification scale and proton lifetime while the GUT-threshold effects on $\sin^2\theta_W$ or M_P have exactly vanishing contribution [53, 54, 57]. This advantage is utilised to estimate GUT-threshold effect on proton lifetime which brings the minimal model prediction closer to planned search limits whereas the prediction with a lighter bi-triplet is found to be already close to the Super K. limit even without GUT threshold effects.

In the case of $0\nu\beta\beta$ decay we analyse the existing data [7–10] on half-life or effective mass parameter using combined contributions of light and sterile neutrino exchanges in the $W_L - W_L$ channel. We derive a new formula for half-life in terms of heavy sterile neutrino masses and provide line plots, band plots, and scattered plots including light neutrino masses of different hierarchies: NH, IH, Planck1, or QD type. Available experimental data including the Hiedelberg-Moscow values are found to be in agreement with the model predictions irrespective of the light neutrino mass hierachies leading to the lower bond on the lightest sterile neutrino mass $\hat{M}_{S_1} > 18.0 \pm 2.9$ GeV. Because of opposite signs of the light and sterile neutrino contributions, cancellation in the combined effective mass or half life is noted to occur when all Majorana phases are neglected for larger (smaller) values of the exchanged sterile neutrino mass $\hat{M}_{S_1}$ when the light neutrino mass is smaller (larger). These results and bounds on the mass of $\hat{M}_{S_1}$ derived here are also applicable to the model of ref. [39] for large W_R boson masses.

We have also investigated the non-SUSY SO(10) symmetry breaking through the flipped $\text{SU}(5) \times \tilde{\text{U}}(1)$ path whose importance has been revived recently [117] in the context of Witten mechanism [116] for radiative generation of RH neutrino masses. As a new realization along this path, we show for the first time how the two gauge couplings of the $\text{SU}(5)\times\tilde{\text{U}}(1)$ gauge symmetry are successfully merged into the SO(10) gauge coupling at the GUT scale although in this case additional fine-tuning has to be adopted to make certain scalar degrees of freedom substantially lighter than the GUT scale. We find possibilities of TeV scale Z', gauged inverse seesaw mechanism for light neutrino masses, and predictions on experimentally testable $0\nu\beta\beta$ decay through heavy sterile neutrino exchanges in the $W_L - W_L$ channel. The lower bound on the lightest sterile neutrino mass obtained along the Pati-Salam path is also applicable in this case although this model has negligible contribution to $n - \bar{n}$ oscillation. This path is also found to possess a rich structure for varieties of charged lepton flavor violations.

This paper is organized in the following manner. In section 2 we discuss the specific SO(10) symmetry breaking chain and study predictions of different physically relevant mass scales emerging as solutions to renormalization group equations. In section 3 we discuss predictions of proton lifetime accessible to ongoing search experiments. Lower bound on the lepto-quark gauge boson mediating rare-kaon decay is derived in section 4 where mixing

JHEP01(2015)045

times for $n-\bar{n}$ oscillation are also predicted. In section 5 we discuss the derivation of Dirac neutrino mass matrix from GUT-scale fit to the charged fermion masses where, in a minimal SO(10) structure, we also show how the model predicts the RH neutrino mass eigenvalues which can be detected at the LHC. Fits to the neutrino oscillation data are discussed in section 6. In section 7 we discuss the model estimations of LFV decay branching ratios and CP-violating parameter due to non-unitarity effects. In section 8 we obtain the model estimations on the dominant contributions to $0\nu\beta\beta$ process and study variation of half-life as a function of sterile neutrino masses. The symmetry breaking through flipped $\mathrm{SU}(5)\times\tilde{U}(1)$ path predicting TeV scale Z' has been discussed in section 9. The LFV and LNV in flipped $\mathrm{SU}(5)\times\tilde{U}(1)$ model are discussed in section 10. The paper is summarized with conclusions in section 11. In the appendix we derive analytic formulas for GUT threshold effects on $\ln(M_P/M_Z)$ and $\ln(M_U/M_Z)$. Scalar multiplets and the gauge running beta coefficients upto two loops for SO(10) symmetry breaking path through Pati-Salam symmetry are also tabulated at the end of appendix.

2 Precision gauge coupling unification and mass scales in SO(10)

In the conventional approach to gauge coupling unification, usually the semi simple gauge symmetry to which the GUT gauge theory breaks is a product of three or four individual groups. As a result the symmetry below the GUT scale involves three or four gauge couplings. The most popular of such examples is $\mathrm{SO}(10)\to G_I$ where $G_I=\mathrm{SU}(2)_L\times\mathrm{U}(1)_Y\times\mathrm{SU}(3)_C$ which has three different gauge couplings, g_Y, g_{2L} and g_{3C}, whose renormalization group (RG) evolution creates a triangular region around the projected unification scale making the determination of the scale more or less uncertain. Even though the region of uncertainty is reduced in the presence of intermediate scales, it exists in principle when, for example, $G_I=\mathrm{SU}(2)_L\times\mathrm{SU}(2)_R\times\mathrm{U}(1)_{B-L}\times\mathrm{SU}(3)_C(\equiv G_{2213})$, that included three or four gauge couplings.[1]

Only in the case when $G_I=\mathrm{SU}(2)_L\times\mathrm{SU}(2)_R\times\mathrm{SU}(4)_C\times D$, the Pati-Salam symmetry with LR discrete symmetry [22] ($\equiv$ D-Parity) [34, 35], there are two gauge couplings $g_{2L}=g_{2R}$ and g_{4C}, and the meeting point of the two RG-evolved coupling lines determines the unification point exactly. As against the apprehended futility in precision SO(10) grand unification [52], several interesting consequences of this intermediate symmetry have been derived earlier including vanishing corrections to GUT-threshold effects on $\sin^2\theta_W$ and the intermediate scale [53, 54, 57, 58]. We find this symmetry to be essentially required at the highest intermediate scale in the present model to guarantee several observable phenomena as SO(10) model predictions while safeguarding precision unification.

We consider the symmetry breaking chain of non-SUSY SO(10) GUT which gives a rich structure of new physics beyond the SM provided the Pati-Salam symmetry occurs as an intermediate symmetry twice: once between the high parity breaking scale (M_P) and the GUT scale (M_U) and, for the second time, without parity between the $\mathrm{SU}(4)_C$ breaking

[1] Very recently unification of gauge couplings with direct breaking to TeV scale G_{2213} has been implemented by utilising a number of light scalar degrees of freedom [123] which may be permitted by resorting to additional fine-tuning of parameters in the Higgs potential.

JHEP01(2015)045

scale (M_C) and M_P

$$\begin{aligned}
\mathrm{SO}(10) &\xrightarrow{M_U} \mathrm{SU}(2)_L \times \mathrm{SU}(2)_R \times \mathrm{SU}(4)_C \times D && [G_{224D},\, g_{2L} = g_{2R}] \\
&\xrightarrow{M_P} \mathrm{SU}(2)_L \times \mathrm{SU}(2)_R \times \mathrm{SU}(4)_C && [G_{224},\, g_{2L} \neq g_{2R}] \\
&\xrightarrow{M_C} \mathrm{SU}(2)_L \times \mathrm{U}(1)_R \times \mathrm{U}(1)_{(\mathrm{B-L})} \times \mathrm{SU}(3)_C && [G_{2113}] \\
&\xrightarrow{M_R} \mathrm{SU}(2)_L \times \mathrm{U}(1)_Y \times \mathrm{SU}(3)_C && [G_{\mathrm{SM}}] \\
&\xrightarrow{m_W} \mathrm{U}(1)_{\mathrm{em}} \times \mathrm{SU}(3)_C && [G_{13}]\,.
\end{aligned}$$

The first step of spontaneous symmetry breaking is implemented by giving GUT scale VEV to the D-Parity even Pati-Salam singlet contained in $54_H \subset \mathrm{SO}(10)$ leading to the left-right symmetric gauge group G_{224D} with the equality in the corresponding gauge couplings $g_{2L} = g_{2R}$. The second step of breaking occurs by assigning Parity breaking VEV to the D-Parity odd singlet $\eta(1,1,1) \subset 210_H$ [34, 35] resulting in the LR asymmetric gauge theory $G_{224}(g_{2L} \neq g_{2R})$. The third step of breaking to gauge symmetry G_{2113} is implemented by assigning VEV of order $M_C \sim 10^5 - 10^6\,\mathrm{GeV}$ to the neutral component of the G_{224} sub-multiplet $(1,3,15) \subset 210_H$. This technique of symmetry breaking to examine the feasibility of observable $n-\bar{n}$ through the type of intermediate breaking $G_{224} \to G_{2113}$ was proposed at a time when neither the neutrino oscillation data, nor the precision CERN-LEP data were available [35–37]. The gauge symmetry G_{2113} that is found to survive down to the TeV scale is broken to the SM by the sub-multiplet $\Delta_R(3,1,\bar{10}) \subset 126_H$ leading to the low-mass extra Z' boson accessible to LHC. At this stage RH Majorana mass matrix $M_N = f\,\langle \Delta_R^0 \rangle$ is generated through the Higgs Yukawa interaction. The last step of breaking occurs as usual through the VEV of the SM doublet contained in the sub-multiplet $\phi(2,2,1) \subset 10_H$. The VEV of the neutral component of RH Higgs doublet $\chi_R(1,2,4)$ under G_{224} symmetry contained in $16_H \subset \mathrm{SO}(10)$ is used to generate the $N-S$ mixing mass term needed for extended seesaw mechanism. For the sake of fermion mass fit at the GUT-scale we utilize two Higgs doublets for $\mu \geq 5\,\mathrm{TeV}$. Out of these two, the up type doublet $\phi_u \subset 10_{H_1}$ contributes to Dirac masses for up quarks and neutrinos, and the down type doublet $\phi_d \subset 10_{H_2}$ contributes to masses of down type quarks and charged leptons. We will see later in this work how the induced VEV of the sub-multiplet $\xi(2,2,15) \subset 126_H$ [39, 85] naturally available in this model plays a crucial role in splitting quark and lepton masses at the GUT scale and determining the value of M_D. In one interesting scenario, the GUT scale fit to fermion masses and mixings results in the diagonal structure of RH neutrino mass matrix near the TeV scale which is accessible for verification at LHC energies.

Using extended survival hypothesis [26, 28] the Higgs scalars responsible for spontaneous symmetry breaking and their contributions to $\beta-$function coefficients up to two-loop order are given in table 6 of appendix A. One set of allowed solutions for mass scales and GUT-scale fine-structure constant is

$$\begin{aligned}
&M_R^0 = 5\,\mathrm{TeV}, \qquad M_\Delta = M_C = 10^{5.5} - 10^{6.5}\,\mathrm{GeV}, \quad M_P = 10^{13.45}\,\mathrm{GeV}, \\
&M_U = 10^{16.07}\,\mathrm{GeV}, \quad \alpha_G = 0.0429.
\end{aligned} \tag{2.1}$$

JHEP01(2015)045

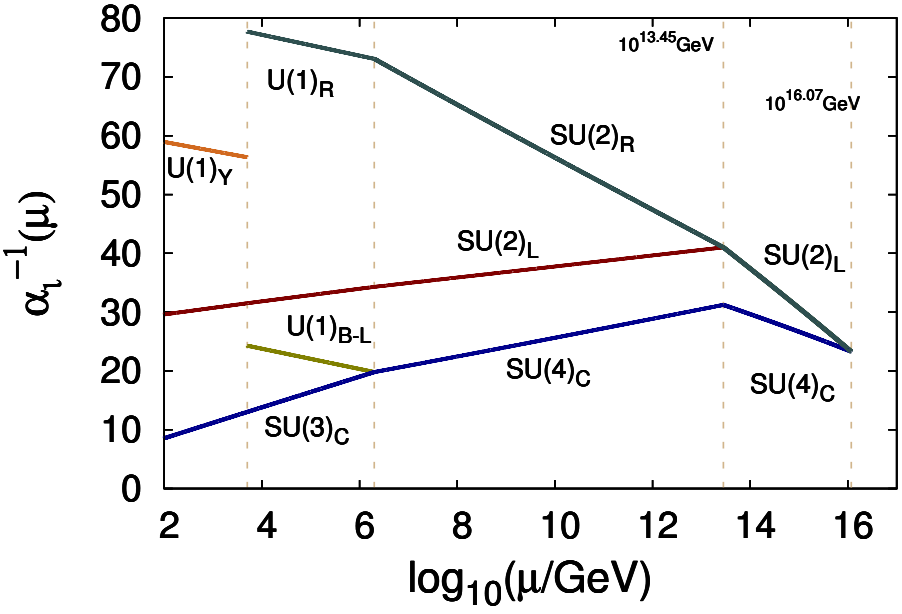

Figure 1. Gauge coupling unification including $\xi(2,2,15)$.

where M_Δ represents the degenerate mass of diquark Higgs scalars contained in $\Delta_R(1,3,\bar{10}) \subset 126_H$.

The renormalization group evolution of gauge couplings is shown in figure 1 exhibiting precision unification.

We have noted that when $M_\Delta < M_C$, there is a small decrease in the unification scale that is capable of reducing the proton lifetime predictions by a factor $3-5$. One example of this solution is,

$$\begin{aligned} &M_R^0 = 5\,\text{TeV}, \qquad M_\Delta = 10^4\,\text{GeV}, \quad M_C = 10^6\,\text{GeV}, \quad M_P = 10^{12.75}\,\text{GeV}, \\ &M_U = 10^{15.92}\,\text{GeV}, \quad \alpha_G = 0.0429. \end{aligned} \tag{2.2}$$

It is interesting to note that the present LHC bound on the diquark Higgs scalar mass [86] is

$$(M_\Delta)_{\text{expt.}} \geq 3.75\text{TeV}. \tag{2.3}$$

As discussed in the context of $n-\bar{n}$ oscillation in section 4, our model accommodates a TeV scale diquark with observable mixing time. But substantial decrease in the unification scale and the corresponding decrease in proton lifetime is possible when the bi-triplet Higgs scalar $\mathbf{\Theta}_H(3,3,1) \subset 54_H$ is lighter than the GUT scale by a factor ranging from $\frac{1}{15} - \frac{1}{25}$. These solutions are discussed in the following section.

3 Low mass Z' and proton decay

3.1 Low-mass Z' boson

In the solutions of RGEs with precision unification, we have found that $g_{(B-L)} = 0.72-0.75$ and $g_{1R} = 0.40-0.42$ in the range of values $M_R^0 = v_{B-L} = 3-10\,\text{TeV}$. This predicts the

JHEP01(2015)045

mass of the Z' boson in the range

$$M_{Z'} = 1.75 - 6.1\,\text{TeV}, \tag{3.1}$$

whereas the current experimental bound from LHC is $(M_{Z'})_{\text{expt.}} \geq 2.5\,\text{TeV}$. Thus, if such a Z' boson in the predicted mass range of the present model exists, it is likely to be discovered by the ongoing searches at the LHC.

3.2 Proton lifetime for $p \to e^+\pi^0$

3.2.1 Predictions at two-loop level

The formula for the inverse of proton-decay width [87–89] is

$$\Gamma^{-1}(p \to e^+\pi^0) = \frac{64\pi f_\pi^2}{m_p}\left(\frac{M_U{}^4}{g_G{}^4}\right)\frac{1}{|A_L|^2|\bar{\alpha_H}|^2(1+D+F)^2 \times R}\,, \tag{3.2}$$

where $R = [(A_{SR}^2 + A_{SL}^2)(1+|V_{ud}|^2)^2]$ for SO(10), $V_{ud} = 0.974 =$ the $(1,1)$ element of V_{CKM} for quark mixings, $A_{SL}(A_{SR})$ is the short-distance renormalization factor in the left (right) sectors and $A_L = 1.25 =$ long distance renormalization factor. $M_U =$ degenerate mass of 24 superheavy gauge bosons in SO(10), $\bar{\alpha}_H =$ hadronic matrix element, $m_p =$ proton mass $= 938.3\,\text{MeV}$, $f_\pi =$ pion decay constant $= 139\,\text{MeV}$, and the chiral Lagrangian parameters are $D = 0.81$ and $F = 0.47$. Here $\alpha_H = \bar{\alpha_H}(1+D+F) = 0.012\,\text{GeV}^3$ is obtained from lattice gauge theory computations. In our model, the product of the short distance with the long distance renormalization factor $A_L = 1.25$ turns out to be $A_R \simeq A_L A_{SL} \simeq A_L A_{SR} \simeq 3.20$. Then using the the two-loop value of the unification scale and the GUT coupling from eq. (2.1) gives

$$\tau_p(p \to e^+\pi^0) \simeq 5.05 \times 10^{35}\text{yrs} \tag{3.3}$$

whereas the solution of RGEs corresponding to eq. (2.2) gives

$$\tau_p(p \to e^+\pi^0) \simeq 1.05 \times 10^{35}\text{yrs}\,. \tag{3.4}$$

For comparison we note the current experimental search limit from Super-Kamiokande is [90, 97–99]

$$(\tau_p)_{\text{SuperK.}} \geq 1.4 \times 10^{34}\text{yrs}\,. \tag{3.5}$$

A second generation underground water cherenkov detector being planned at Hyper-Kamiokande in Japan is expected to probe higher limits through its 5.6 Megaton year exposure leading to the partial lifetime [99]

$$(\tau_p)_{\text{HyperK.}} \geq 1.3 \times 10^{35}\text{yrs}\,. \tag{3.6}$$

Thus our model prediction in eq. (3.4) barely within the planned Hyper-K limit although the prediction in eq. (3.3) nearly 4 times larger than this limit.

If the proton decay is observed closer to the current or planned experimental limits, it would vindicate the long standing fundamental hypothesis of grand unification. On the other hand proton may be much more stable and its lifetime may not be accessible even to Hyper K. experimental search programme. These possibilities are addressed below.

JHEP01(2015)045

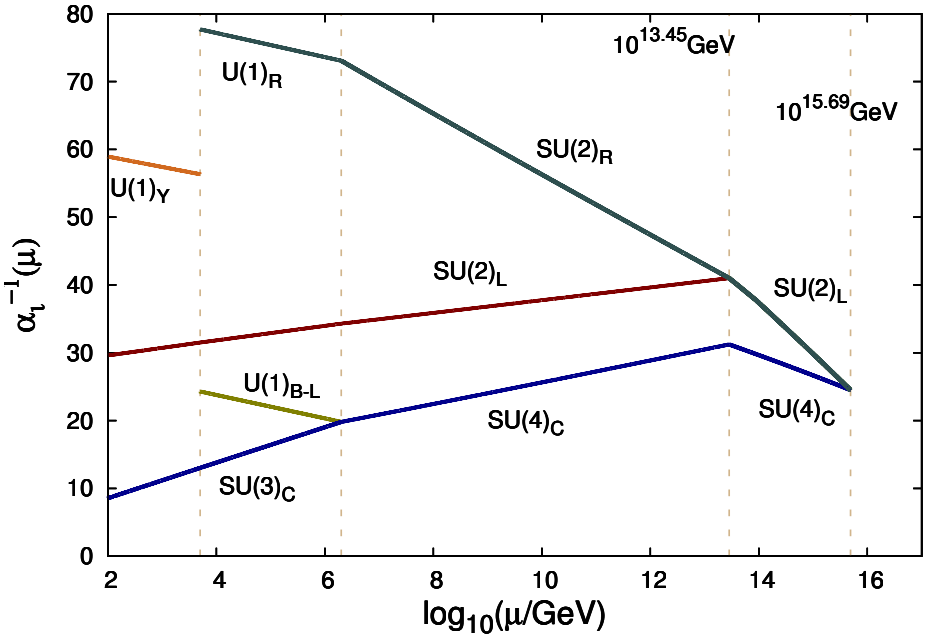

Figure 2. Same as figure 1 but with the Higgs scalar bi-triplet of mass 9×10^{13} GeV.

3.2.2 GUT scale and proton life-time reduction through bi-triplet scalar

We note that the present estimation of the GUT scale can be significantly lowered so as to bring the proton-lifetime prediction closer to the current Super-K. limit if the the Higgs scalar bi-triplet $\mathbf{\Theta}_H(3,3,1) \subset 54_H$ of SO(10) is near the Parity violating intermediate scale. For example in figure 2, we have shown how in this model only the unification scale is lowered while keeping the other physical mass scales unchanged as in eq. (2.1) for a value of $M_{331} = 9 \times 10^{13}$ GeV.

In table 1 we have presented various allowed values of the GUT scale and the proton life-time for different combinations of the diquark Higgs scalar masses M_Δ contained in $\Delta_R(1,3,\bar{10}) \subset 126_H$ which mediate $n - \bar{n}$ oscillation process. Even for a bi-triplet mass $M_U/15$ we note a reduced value of the unification scale at $M_U = 10^{15.63}$ GeV and the corresponding proton lifetime at $\tau_P = 4.6 \times 10^{33}$ yrs when $M_\Delta \sim 10^4$ GeV. The estimated lifetimes without including the GUT-threshold effects is found to be in the range $\tau_P = 4.6 \times 10^{33}$ yrs to 2.1×10^{35} yrs, most of which are between the Super-K and the Hyper-K limits.

An important source of uncertainty on τ_P in GUTs is known to be due to GUT-threshold effects as illustrated in the following sub-section.

3.2.3 Estimation of GUT-threshold effects

That there could be significant threshold effects on the unification scale arising out of heavy and super-heavy particle masses was pointed out especially in the context of grand desert models [48, 49, 51, 56] and in intermediate scale SO(10) models [53–55, 57–64].

JHEP01(2015)045

M_Δ (GeV)	M_P (GeV)	$M_{(3,3,1)}$ (GeV)	M_U (GeV)	α_G^{-1}	τ_p(years)
$10^{4.0}$	$10^{12.73}$	$10^{14.00}$	$10^{15.57}$	22.37	4.65×10^{33}
$10^{4.0}$	$10^{12.73}$	$10^{14.50}$	$10^{15.66}$	22.08	1.03×10^{34}
$10^{4.0}$	$10^{12.73}$	$10^{15.00}$	$10^{15.75}$	21.79	2.32×10^{34}
$10^{4.0}$	$10^{12.73}$	$10^{15.92}$	$10^{15.92}$	21.22	1.05×10^{35}
$10^{4.5}$	$10^{12.89}$	$10^{14.00}$	$10^{15.60}$	23.16	6.58×10^{33}
$10^{4.5}$	$10^{12.89}$	$10^{14.50}$	$10^{15.69}$	22.88	1.47×10^{34}
$10^{4.5}$	$10^{12.89}$	$10^{15.50}$	$10^{15.87}$	22.19	7.26×10^{34}
$10^{4.5}$	$10^{12.89}$	$10^{15.95}$	$10^{15.95}$	22.01	1.49×10^{35}
$10^{5.0}$	$10^{13.05}$	$10^{14.00}$	$10^{15.62}$	23.94	8.45×10^{33}
$10^{5.0}$	$10^{13.05}$	$10^{14.50}$	$10^{15.71}$	23.66	1.89×10^{34}
$10^{5.0}$	$10^{13.05}$	$10^{15.50}$	$10^{15.89}$	23.08	9.44×10^{34}
$10^{5.0}$	$10^{13.05}$	$10^{15.98}$	$10^{15.98}$	22.79	2.11×10^{35}

Table 1. Predictions on lifetime for the decay $p \to e^+\pi^0$ with lower values of masses of the bi-triplet and the diquark Higgs scalars.

In order to examine how closer to or farther from the current experimental bound our model predictions could be, we have estimated the major source of uncertainty on proton lifetime due to GUT threshold effects in SO(10) with intermediate scales [58, 59] taking into account the contributions of the superheavy (SH) components in $54_H, 126_H, 210_H, 10_{H_1}$ and 10_{H_2} in the case of the minimal model

$$\begin{aligned} 210_H &\supset \Sigma_1(2,2,10) + \Sigma_2(2,2,\overline{10}) + \Sigma_3(2,2,6) + \Sigma_4(1,1,15), \\ 54_H &\supset S_1(1,1,20 + S_2(3.3,1) + S_3(2,2,6), \\ 126_H &\supset \Delta_1(1,1,6), \qquad 10_{H_i} \supset H_i(1,1,6), i = 1,2, \end{aligned} \tag{3.7}$$

where the quantum numbers on the r.h.s. are under the gauge group G_{224} and the components have superheavy masses around the GUT scale. It was shown in refs. [53, 54, 57] that when G_{224D} occurs as intermediate symmetry, all loop corrections due to superheavy masses $m_{SH} \geq M_P$ cancels out from the predictions of $\sin^2\theta_W$ and also from M_P obtained as solutions of RGEs for gauge couplings while the GUT threshold effect on the unification scale due to the superheavy scalar masses assumes an analytically simple form. As outlined in the appendix, even in the presence of two more intermediate symmetries below M_P, analogous formulas on the GUT-threshold effects are also valid

$$\Delta \ln\left(\frac{M_{\rm U}}{M_{\rm Z}}\right) = \frac{\lambda^U_{2L} - \lambda^U_{4C}}{6(a'''_{2L} - a'''_{4C})} \tag{3.8}$$

where a'''_i is one-loop beta function coefficients in the range $\mu = M_P - M_U$ for the gauge

JHEP01(2015)045

group G_{224D}. In eq. (3.8)

$$\lambda_i^U = b_i^V + \Sigma_{\rm SH} b_i^{\rm SH} \ln\left(\frac{M_{SH}}{M_U}\right), \quad i = 2L, 2R, 4C \tag{3.9}$$

$b_i^V = tr(\theta_i^V)^2$ and $b_i^{\rm SH} = tr(\theta_i^{\rm SH})^2$ where θ_i^V ($\theta_i^{\rm SH}$) are generators of the gauge group G_{224D} in the representations of superheavy gauge bosons (Higgs scalars). The one-loop coefficients for various SH components in eq. (3.7) contributing to threshold effects are [58]

$$\begin{aligned}
&b_{2L}^V = b_{2R}^V = 6, && b_{4C}^V = 4, && b_i^{\Sigma_4} = (0,0,4)\\
&b_i^{\Sigma_1} = b_i^{\Sigma_2} = (10,10,12), && b_i^{\Sigma_3} = b_i^{S_3} = (6,6,4), &&\\
&b_i^{S_1} = (0,0,16), && b_i^{S_2} = (12,12,0), && b_i^{H_{1,2}} = b_i^{\Delta_1} = (0,0,2),
\end{aligned} \tag{3.10}$$

where we have projected out the would-be Goldstone components from S_3 leading to

$$\lambda_{2L}^U - \lambda_{4C}^U = 2 - 6\eta_{210} - 2\eta_{54} - 2\eta_{126} - 4\eta_{10}, \tag{3.11}$$

with $\eta_X = \ln(M_X/M_U)$, and we have made the plausible assumption that all SH scalars belonging to a particular SO(10) representation have a common mass such as $M_{210} = M_{\Sigma_i} (i = 1-4)$ for 210_H and so on for other representations [59]. Utilising the model coefficients $a_{2L}''' = 44/3$ and $a_{4C}''' = 16/3$, and using eq. (3.11) in eq. (3.8) gives

$$M_U/M_U^0 = 10^{(0.25\ln\eta)/2.3025} \tag{3.12}$$

where $\eta = 10(1/10)$ depending upon our assumption that SH components are 10(1/10) times heavier(lighter) than the GUT scale. By applying these GUT-threshold effects to the solutions of RGE in eq. (2.2), we obtain

$$\begin{aligned}
M_U &= 10^{15.92\pm0.25}\,\text{GeV},\\
\tau_p(p\to e^+\pi^0) &\simeq 5.05\times 10^{35\pm1.0\pm0.34}\text{yrs}
\end{aligned} \tag{3.13}$$

where the first uncertainty is due to GUT threshold effects, and the second uncertainty, derived in appendix, is due to the 1σ level uncertainties in the experimental values of $\sin^2\theta_W(M_Z)$ and $\alpha_S(M_Z)$. It is clear from eq. (3.13) that our prediction covers wider range of values in proton lifetime prediction including those few times larger than the current Super-K. limit.

Similarly each of the numerical values in the last column of table 1 is modified by this additional uncertainty factor of $10^{\pm1\pm0.32}$ in the estimated lifetimes.

4 Rare kaon decay and $n-\bar{n}$ oscillation

In this section we discuss the model predictions on rare kaon decays mediated by lepto-quark gauge bosons of $SU(4)_C$ that occurs as a part of Pati-Salam intermediate gauge symmetry $SU(2)_L \times SU(2)_R \times SU(4)_C$ which undergoes spontaneous symmetry breaking at the mass scale $\mu = M_R^+ = M_C$ to G_{2113} which in turn breaks to SM generating the TeV scale Z' boson. The lepto-quark Higgs scalar contribution to the rare decay process is suppressed in this model due to the natural values of their masses at $M_C = 10^6$ GeV and smaller Yukawa couplings.

JHEP01(2015)045

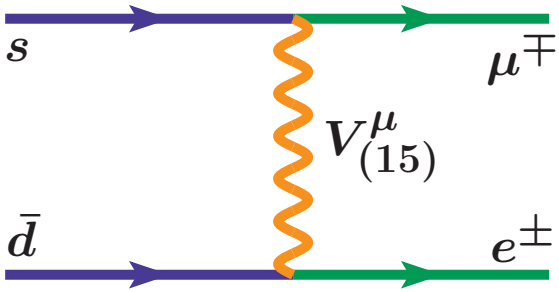

Figure 3. Feynman diagram for rare kaon decays $K_L^0 \to \mu^{\pm} e^{\mp}$ mediated by a heavy lepto-quark gauge boson of $SU(4)_C$ gauge symmetry.

4.1 Rare kaon decay $K_L \to \mu\bar{e}$

Earlier several attempts have been made to derive lower bound on the lepto-quark gauge boson mass [22, 91–93]. In this sub-section using the symmetry breaking $G_{224} \to G_{2113} \to SM$ consistent with an observable Z' boson and the improved bound on the rare kaon decay branching ratio [38], we update the existing lower bound on the $SU(4)_C$-leptoquark gauge boson mass which was estimated [93] using the direct breaking $G_{224} \to SM$ and then existing experimental upper bound on the branching ratio [94]

$$\text{Br.}\left(K_L \to \mu\bar{e}\right)_{\text{expt.}} \equiv \frac{\Gamma\left(K_L \to \mu^{\pm} e^{\mp}\right)}{\Gamma\left(K_L \to \text{all}\right)} < 10^{-10.28}\,. \tag{4.1}$$

This measurement which was improved later by one order by BNL collaboration gives [38]

$$\text{Br.}\left(K_L \to \mu\bar{e}\right)_{\text{expt.}} < 4.7 \times 10^{-12}. \tag{4.2}$$

While all earlier derivations were made assuming direct breaking of Pati-Salam model to the SM, in this work we include the intermediate breaking G_{2113} symmetry corresponding to the presence of TeV scale Z' boson. Thus our renormalization group equations are different and numerical value arrived is much more precise. While the central value of the bound is nearly two times larger, its uncertainty is drastically reduced compared to the earlier results. We have further noted that if G_{2113} symmetry is replaced by G_{2213} as in the model of [39], the results are not significantly affected.

The leptoquark gauge bosons of $SU(4)_C$ in the adjoint representation $(1, 1, 15)$ under G_{224} mediate rare kaon decay $K_L \to \mu^{\pm} e^{\mp}$ whose Feynman diagram is shown in the figure 3. Analytic formulas for the corresponding branching ratio is [92, 93],

$$\text{Br.}\left(K_L \to \mu\bar{e}\right) = \frac{4\pi^2 \alpha_s^2(M_C)\, m_K^4\, R}{G_F^2 \sin^2\theta_C m_\mu^2 (m_s + m_d)^2\, M_C^4}, \tag{4.3}$$

where the factor R includes renormalization effects on the quark masses m_d or m_s from $\mu = M_C$ down to $\mu = \mu_0 = 1\,\text{GeV}$ through the G_{2113}, the SM and the $SU(3)_C$ gauge symmetries.

JHEP01(2015)045

Noting that the down quark or the strange quark mass satisfies the following renormalization group equations,

$$m_{d,s}(M_C) = \frac{m_{d,s}(\mu_0)}{\eta_{\rm em}} R_{2113} R^{(6)}_{213} R^{(5)}_{213} R^{(5)}_{\rm QCD} R^{(4)}_{\rm QCD} R^{(3)}_{\rm QCD} \tag{4.4}$$

where

$$\begin{aligned}
R_{2113} &= \Pi_i \left(\frac{\alpha_i(M_C)}{\alpha_i(M_R^0)}\right)^{-C_1^i/2a_i^{(1)}}, \qquad i = 2L, 1R, B-L, 3_C\,, \\
R^{(6)}_{213} &= \Pi_i \left[\frac{\alpha_i(M_{R^0})}{\alpha_i(m_t)}\right]^{-C_2^i/2a_i^{(2)}}, \qquad R^{(5)}_{213} = \Pi_i \left[\frac{\alpha_i(m_t)}{\alpha_i(M_Z)}\right]^{-C_2^i/2a_i^{(3)}}, \quad i = 2L, Y, 3C\,, \\
{R^{(5)}}_{\rm QCD} &= \left[\frac{\alpha_S(M_Z)}{\alpha_S(m_b)}\right]^{-4/a^{(4)}}, \qquad {R^{(4)}}_{\rm QCD} = \left[\frac{\alpha_S(m_b)}{\alpha_i(m_c)}\right]^{-4/a^{(5)}} \\
{R^{(3)}}_{QCD} &= \left[\frac{\alpha_S(m_c)}{\alpha_S(\mu^0)}\right]^{-4/a^{(6)}}.
\end{aligned} \tag{4.5}$$

Here the input parameters used in above eq. (4.5) are: $C_1^i = (0, 0, 1/4, 8)$, $C_2^i = (0, -1/5, 8)$ and the one-loop beta-coefficients relevant for our present work are $a_i^{(1)} = (-3, 57/12, 37/8, -7)$, $a_i^{(2)} = (-19/6, 41/10, -7)$, $a_i^{(3)} = (-23/6, 103/30, -23/3)$, $a^{(4)} = -23/3$, $a^{(5)} = -25/3$, $a^{(6)} = -9$. Now we can obtain the renormalization factor in eq. (4.3)

$$R = \left[R_{2113} R^{(6)}_{213} R^{(5)}_{213} R^{(5)}_{QCD} R^{(4)}_{QCD} R^{(3)}_{QCD}\right]^{-2}. \tag{4.6}$$

Using eq. (4.5) and eq. (4.6) and eq. (4.2), we derive the following inequality,

$$F_L(M_C, M_R^0) > \left[\frac{4\pi^2 m_K^4 R_p}{G_F^2 \sin^2\theta_C m_\mu^2 (m_s + m_d)^2} \times 10^{11.318}\right]^{1/4}, \tag{4.7}$$

where

$$\begin{aligned}
F_L(M_C, M_R^0) &= M_C \alpha_S^{-3/14}(M_C) \alpha_Y^{-1/82}(M_{R^0}) \left[\frac{\alpha_{B-L}(M_C)}{\alpha_{B-L}(M_{R^0})}\right]^{-1/74} \alpha_Y^{1/82}(m_t) \alpha_C^{-2/7}(m_t), \\
R_p &= \left[R^{(5)}_{213} R^{(5)}_{QCD} R^{(4)}_{QCD} R^{(3)}_{QCD}\right]^{-2}.
\end{aligned} \tag{4.8}$$

In figure 4 the function $F_L(M_C, M_R^0)$ in the l.h.s. of eq. (4.7) is plotted against M_C for a fixed value of $M_R^0 = 5\,\text{TeV}$, where the Horizontal lines represent the r.h.s. of the same equation including uncertainties in the parameters. Thus, for the purpose of this numerical estimation, keeping M_R^0 fixed at any value between $5 - 10\,\text{TeV}$, we vary M_C until the l.h.s. of eq. (4.7) equals its r.h.s..

For our computation at $\mu_0 = 1\,\text{GeV}$, we use the inputs $m_K = 0.4976\,\text{GeV}$, $m_d = 4.8^{+0.7}_{-0.3}\,\text{MeV}$, $m_s = 95 \pm 5\,\text{MeV}$, $m_\mu = 105.658\,\text{MeV}$, $G_F = 1.166 \times 10^{-5}\,\text{GeV}^{-2}$, and $\sin\theta_C = 0.2254 \pm 0.0007$, $m_b = 4.18 \pm 0.03\,\text{GeV}$, $m_c = 1.275 \pm 0.025\,\text{GeV}$, $m_t = 172\,\text{GeV}$. At $\mu = M_Z$ we have used $\sin^2\theta_W = 0.23166 \pm 0.00012$, $\alpha_S = 0.1184 \pm 0.0007$, $\alpha^{-1} = 127.9$

JHEP01(2015)045

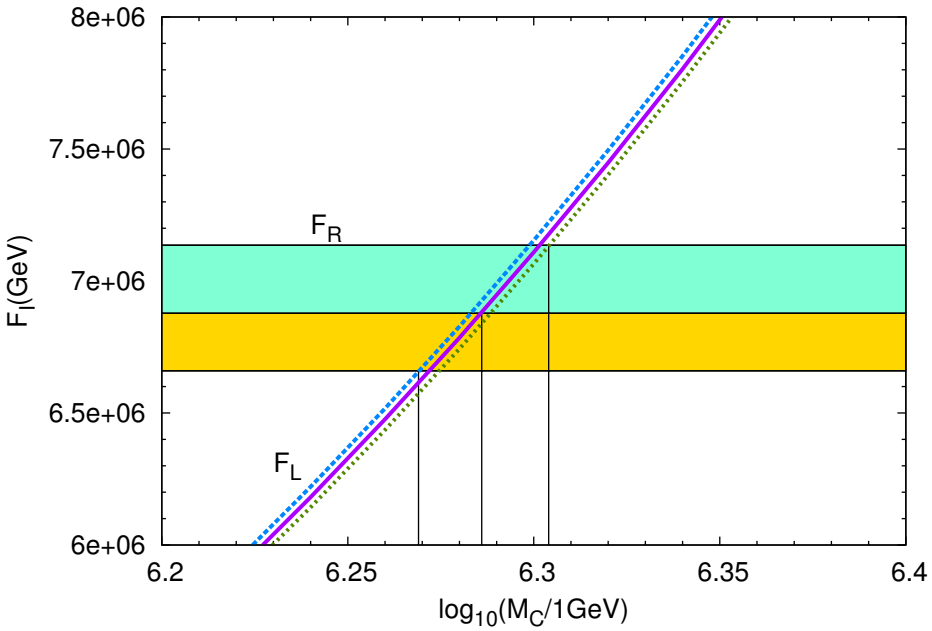

Figure 4. Graphical representation of the method for numerical solution of the lower bound on M_C. The horizontal lines are the r.h.s. of the inequality (4.7) whereas the curve represents the l.h.s.. The colored horizontal bands are due to uncertainties in the input parameters.

and utilized eq. (4.2)−eq. (4.8). With $M_{R^0} = 5\,\text{TeV}$ and $M_{Z'} \simeq 1.2\,\text{TeV}$, the existing experimental upper bound on Br.$(\text{K}_L \to \mu^{\mp}e^{\pm})$ gives the lower bound on the G_{224} symmetry breaking scale

$$M_C > (1.932^{+0.082}_{-0.074}) \times 10^6\,\text{GeV}. \tag{4.9}$$

Noting from figure 1 that in our model $\alpha_S(M_C) = 0.0505$, we get from eq. (4.9) as rare-kaon decay constraint on the $\text{SU}(4)_C$ lepto-quark gauge boson mass

$$M_{\text{LQ}} > (1.539^{+0.065}_{-0.059}) \times 10^6\,\text{GeV}. \tag{4.10}$$

where the uncertainty is due to the the existing uncertainties in the input parameters. From the derived solutions to RGEs for gauge couplings this lower bound on the lepto-quark gauge boson mass is easily accommodated in our model. The new results obtained in this analysis is compared to the earlier results including those in refs. [22, 91–93] as shown in table 2.

4.2 Neutron-antineutron oscillation

Here we discuss the prospect of this model predictions for experimentally observable $n-\bar{n}$ oscillation while satisfying the rare-kaon decay constraint by fixing the G_{224} symmetry breaking scale at $M_C \sim 2 \times 10^6\,\text{GeV}$ as derived in eq. (4.9). The Feynman diagrams for the $n-\bar{n}$ oscillation processes are shown in left- and right-panel of figure 5 where $\Delta_{\text{u}^c\text{u}^c}$, $\Delta_{\text{d}^c\text{d}^c}$, and $\Delta_{\text{u}^c\text{d}^c}$ denote different diquark Higgs scalars contained in $\Delta_R(1,3,\overline{10}) \subset 126_H$.

JHEP01(2015)045

Input Br.$(K_L \to \mu\bar{e})$	Sym. Breaking and Corrections used	Derived Bound on $\mathbf{M_{LQ}}$ (GeV)	Ref.
$\frac{\Gamma(K_L\to\mu\bar{e})}{\Gamma(K_L\to\mu^+\mu^-)} < G_F^2\alpha^2$	$G_{224} \to SM$ Tree level	$> 3 \times 10^4$	Pati, Salam [22]
Br.$(K_L \to \mu\bar{e})$ $< 6.25 \times 10^{-10}$	$G_{224} \to SM$ Tree level	$> 3.1 g_{4c} \times 10^5$	Dimopoulos, Raby, Kane [91]
Br.$(K_L \to \mu\bar{e})$ $< 7.6 \times 10^{-10}$	$G_{224} \to SM$ Only QCD	$> 3.5 \times 10^5$	Deshpande, Johnson [92]
Br.$(K_L \to \mu\bar{e})$ $< 10^{-10.28}$	G_{224} or $G_{214} \to SM$ QCD and EW	$> 9.06^{+2.41}_{-1.98} \times 10^5$	Parida, Purkayastha [93]
Br.$(K_L \to \mu\bar{e})$ $< 4.7 \times 10^{-12}$	$G_{224} \to G_{2113} \to SM$ QCD and EW	$> (1.539^{+0.065}_{-0.059}) \times 10^6$	This analysis

Table 2. Predictions of upper bounds on the lepto-quark gauge boson mass $\mathbf{M_{LQ}}$ mediating rare kaon decays and its comparison with earlier results where $\mathbf{M_{LQ}} = g_{4C} V_{G_{224}}$, $V_{G_{224}}$ being the G_{224} symmetry breaking scale.

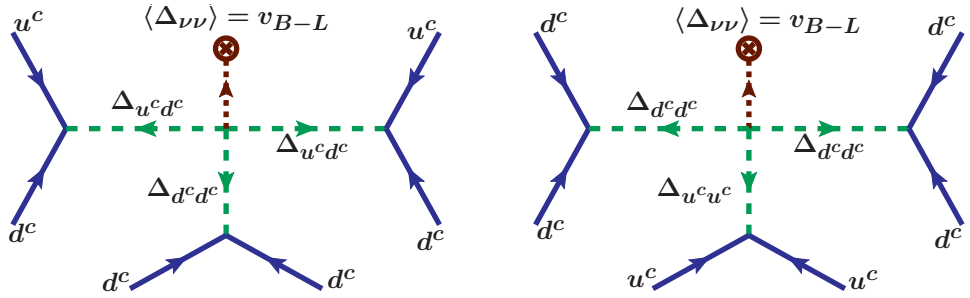

Figure 5. Feynman diagrams for neutron-antineutron oscillation via mediation of two $\Delta_{u^c d^c}$ and one $\Delta_{d^c d^c}$ diquark Higgs scalars as shown in the left-panel while mediation of two $\Delta_{d^c d^c}$ and one $\Delta_{u^c u^c}$ diquark Higgs scalars as shown in the right-panel.

The amplitude for these two diagrams can be written as

$$\text{Amp}^{(a)}_{n-\bar{n}} = \frac{f_{11}^3 \lambda v_{B-L}}{M^4_{\Delta_{u^c d^c}} M^2_{\Delta_{d^c d^c}}}, \quad \text{Amp}^{(b)}_{n-\bar{n}} = \frac{f_{11}^3 \lambda v_{B-L}}{M^4_{\Delta_{d^c d^c}} M^2_{\Delta_{u^c u^c}}}, \tag{4.11}$$

where $f_{11} = (f_{\Delta_{u^c d^c}}) = (f_{\Delta_{d^c d^c}}) = (f_{\Delta_{u^c u^c}})$ from the SO(10) invariance and the quartic coupling between different diquark Higgs scalar has its natural value i.e, $\mathcal{O}(0.1) - \mathcal{O}(1)$.

The $n - \bar{n}$ mixing mass element $\delta m_{n\bar{n}}$ and the dibaryon number violating amplitude $W_{(B=2)} = \text{Amp}^{(a)} + \text{Amp}^{(b)}$ are related up to a factor depending upon combined effects of hadronic and nuclear matrix element effects

$$\delta m_{n\bar{n}} = \left(10^{-4}\,\text{GeV}^6\right) \cdot W_{B=2}. \tag{4.12}$$

JHEP01(2015)045

f_{11}	λ	$M_{\Delta_{u^c d^c}}$ (GeV)	$M_{\Delta_{d^c d^c}}$ (GeV)	$\tau_{\mathrm{n}-\bar{\mathrm{n}}}$ (secs)
0.1	0.1	10^5	10^5	6.6×10^9
0.0236	0.1	10^5	10^5	2.5×10^{13}
0.0236	1.0	10^5	10^5	2.5×10^{14}
0.1	0.1	10^4	10^5	6.6×10^9
0.0236	1.0	10^4	10^5	2.5×10^{13}
0.0236	1.0	10^5	10^4	2.5×10^{13}

Table 3. Predictions for n−n̄ oscillation mixing time as a function of allowed couplings and masses of diquark Higgs scalars in the model described in the text.

The experimentally measurable mixing time $\tau_{\mathrm{n}\bar{\mathrm{n}}}$ is just the inverse of $\delta m_{\mathrm{n}\bar{\mathrm{n}}}$

$$\tau_{\mathrm{n}\bar{\mathrm{n}}} = \frac{1}{\delta m_{\mathrm{n}\bar{\mathrm{n}}}}. \tag{4.13}$$

With $v_{B-L} = 5\,\mathrm{TeV}$ in the degenerate case, when all diquark Higgs scalars have identical masses $M_\Delta = 10^5\,\mathrm{GeV}$, the choice of the parameters $f_{11} \simeq \lambda \sim \mathcal{O}(0.1)$ gives $\tau_{\mathrm{n}\bar{\mathrm{n}}} = 6.58 \times 10^9$ sec. As described below our SO(10) model can fit all charged fermion masses and CKM mixings at the GUT scale with two kinds of structures: (i) only one 126_H, and (ii) two Higgs representations 126_H and $126'_H$. In the minimal case the Yukawa coupling f of 126_H to fermions has a diagonal structure,

$$f = \mathrm{diag}(0.0236, -0.38, 1.5), \tag{4.14}$$

which gives through eq. (4.11), eq. (4.12), and eq. (4.13)

$$\tau_{n-\bar{n}} = 10^8 - 10^{10}\,\mathrm{secs}. \tag{4.15}$$

This model prediction is accessible to ongoing search experiments [95]. However, the GUT scale fit to the fermion masses can be successfully implemented without constraining the f values when a second $126'_H$ is present at the GUT scale with all its component at M_U except $\xi'(2,2,15)$ being around the M_P scale. Then using $f_{11} = 0.1 - 0.01$, the estimated value turns out to be

$$\tau_{n-\bar{n}} \sim 10^9 - 10^{13}\,\mathrm{sec}. \tag{4.16}$$

Out of this the mixing time in the range $10^9 - 10^{10}$ sec can be probed by ongoing experiment [95].

5 Determination of Dirac neutrino mass matrix

The Dirac neutrino mass near the TeV scale forms an essential ingredient in the estimations of inverse seesaw contribution to light neutrino masses and mixings as well as the LFV and LNV processes in this model in addition to predicting leptonic CP-violation through non-unitarity effects. Since the procedure for determination of M_D has been discussed

JHEP01(2015)045

earlier [39], we mention it briefly here in the context of the present model. In order to obtain the Dirac neutrino mass matrix M_D and the RH Majorana mass matrix M_N near TeV scale, at first the PDG values [65] of fermion masses at the electroweak scale are extrapolated to the GUT scale using the renormalization group equations (RGEs) for fermion masses in the presence of the SM for $\mu = M_Z - 5\,\text{TeV}$, and from $\mu = 5 - 10\,\text{TeV}$ using the RGEs in the presence of G_{2113} symmetry [71, 101]. From $\mu = 5 - 100\,\text{TeV}$, RGEs corresponding to two Higgs doublets in the presence of G_{2113} symmetry are used [71]. These two doublets which act like up-type and down type doublets are treated to have originated from separate representations 10_{H_1} and 10_{H_2} of SO(10). For mass scale $\mu \geq 10^5\,\text{GeV}$ till the GUT scale the fermion mass RGEs derived in the presence of the G_{224} and G_{224D} symmetries [72] are exploited. Then at the GUT scale $\mu = M_U$ we obtain the following values of mass eigenvalues and the CKM mixing matrix $m_u^0 = 1.301$ MeV, $m_c^0 = 0.1686\,\text{GeV}$, $m_t^0 = 51.504\,\text{GeV}$, $m_d^0 = 1.163\,\text{MeV}$, $m_s^0 = 23.352$ MeV, $m_b^0 = 1.0256\,\text{GeV}$, $m_e^0 = 0.2168\,\text{MeV}$, $m_\mu^0 = 38.846\,\text{MeV}$, $m_\tau^0 = 0.962\,\text{GeV}$,

$$V_{\text{CKM}}^0(M_{\text{U}}) = \begin{pmatrix} 0.976 & 0.216 & -0.0017 - 0.0035i \\ -0.216 - 0.0001i & 0.976 - 0.0000i & 0.0310 \\ 0.0083 - 0.0035i & -0.03 - 0.0007i & 0.999 \end{pmatrix}. \tag{5.1}$$

Formulas for different fermion mass matrices at the GUT scale have been discussed in [39, 71]

$$\begin{aligned} M_u^0 &= G_u + F, \quad & M_D^0 &= G_u - 3F, \\ M_d^0 &= G_d + F, \quad & M_l &= G_d - 3F, \end{aligned} \tag{5.2}$$

where $G_u = Y_1 v_u, G_d = Y_2 v_d$, and in the absence of 126_H in those models , the diagonal structure of F was shown to originate from available non-renormalizable higher dimensional operators.The new interesting point here is that the present model permits F to be renormalizable using the ansatz [85] $F = f v_\xi$, and the induced VEV v_ξ of $\xi(2,2,15) \subset 126_H$ is predicted within the allowed mass scales of the SO(10) while safeguarding precision gauge coupling unification.

Using the charged-lepton diagonal mass basis and eq. (5.2) we have

$$\begin{aligned} M_e(M_U) &= \text{diag}(0.000216, 0.0388, 0.9620)\,\text{GeV}, \\ G_{d,ij} &= 3F_{ij}, \ (i \neq j). \end{aligned} \tag{5.3}$$

In the present model, type-II seesaw contribution being negligible and the neutrino oscillation data being adequately represented by inverse seesaw formula, there is no compelling reason for the Majorana coupling f to be non-diagonal. On the other hand diagonal texture of RH neutrino mass matrix has been widely used in the literature in a large class of SO(10) models. Moreover, as we see below, the diagonal structure of f which emerges in the minimal model exactly predicts the RH neutrino masses accessible to LHC and the neutrino oscillation data.[2] We then find that diagonal texture of f gives the matrix G_d to

[2]Alternatively the fermion masses at the GUT scale can be fitted by the diagonal coupling f' of a second $126_{H'}$ whose $\xi'(2,2,15)$ component can be fine-tuned to have mass at the same intermediate scale to provide the desired VEV. In this case the f and RH Majorana neutrino mass matrix M_N is allowed to possess a general 3×3 matrix structure without any apriori constraint.

JHEP01(2015)045

be also diagonal leading to the relations

$$\begin{aligned} \mathrm{G_{d,ii}} + \mathrm{F_{ii}} &= m_i^0, \quad (i = d, s, b), \\ \mathrm{G_{d,jj}} - 3\mathrm{F_{jj}} &= m_j^0, \quad (j = e, \mu, \tau). \end{aligned} \tag{5.4}$$

$$\begin{aligned} F &= \mathrm{diag}\frac{1}{4}(m_d^0 - m_e^0, m_s^0 - m_\mu^0, m_b^0 - m_\tau^0), \\ &= \mathrm{diag}(2.365 \times 10^{-4}, -0.0038, +0.015)\,\mathrm{GeV}, \\ G_d &= \mathrm{diag}\frac{1}{4}(3m_d^0 + m_e^0, 3m_s^0 + m_\mu^0, 3m_b^0 + m_\tau^0), \\ &= \mathrm{diag}(9.2645 \times 10^{-4}, 0.027224, 1.00975)\,\mathrm{GeV}, \end{aligned} \tag{5.5}$$

where we have used the RG extrapolated values at the GUT scale. It is clear from the value of the mass matrix F in eq. (5.5) that we need a small VEV $v_\xi \sim 10\,\mathrm{MeV}$ to fit the fermion mass fits at the GUT scale. To verify that this v_ξ is naturally obtained in this model, we note that the spontaneous symmetry breaking in this model $G_{224} \to G_{2113}$ occurs through the VEV of $(1,3,15)_H \subset 210_H$. Then the desired trilinear term in the scalar potential V gives the natural value of the VEV

$$\begin{aligned} V &= \lambda_3 M_U 210_H . 126_H^\dagger 10_H \\ &= \lambda_3 M_U (1,3,15)_{210} . (2,2,15)_{126} . (2,2,1)_{10_{1,2}}, \\ v_\xi &\sim \lambda_3 M_U M_C v_{\mathrm{ew}}/M_\xi^2 = 10\mathrm{MeV} - 100\mathrm{MeV}, \end{aligned} \tag{5.6}$$

for $M_\xi = 10^{12} - 10^{13}\,\mathrm{GeV}$.

Repeating the RG analysis of ref. [39] we have verified that the precision gauge coupling unification is unaffected when $\xi(2,2,15)$ occurs at such high intermediate scales except for an increase of the GUT scale by nearly 2 and the GUT fine structure constant by nearly three times. That the Parity violating scale and the GUT scale would be marginally affected is easy to understand because the contribution due to $\xi(2,2,15)$ to all the three one-loop beta-function coefficients are almost similar $\delta b_{2\mathrm{L}} = \delta b_{2\mathrm{R}} = 5, \delta b_{4\mathrm{C}} = 5.333$. That the unification is bound to occur can be easily seen because there are only two gauge coupling constant lines for $\mu > M_P$.

Using the computed values of M_u^0 and the value of F from eq. (5.5) in eq. (5.2), gives the the matrix G_u at $\mu = M_U$. Another by product of this fermion mass fit at the GUT scale is that the matrix elements of F now gives $f = \mathrm{diag}(f_1, f_2, f_3)$ and consequently the RH neutrino mass hierarchy $M_{N_1} : M_{N_2} : M_{N_3} = 0.023 : -0.38 : 1.5$. This hierarchy is consistent with lepton-number and lepton flavor violations discussed in section 5, section 6, section 7, and section 8.

$$G_u(M_U) = \begin{pmatrix} 0.0095 & 0.0379 - 0.0069i & 0.0635 - 0.1671i \\ 0.0379 + 0.0069i & 0.2637 & 2.117 + 0.0001i \\ 0.0635 + 0.1672i & 2.117 - 0.0001i & 51.444 \end{pmatrix} \mathrm{GeV}\,. \tag{5.7}$$

Now using eq. (5.5) and eq. (5.7) in eq. (5.2) gives the Dirac neutrino mass matrix M_D

JHEP01(2015)045

at the GUT scale

$$M_D^0(M_U) = \begin{pmatrix} 0.00876 & 0.0380 - 0.0069i & 0.0635 - 0.1672i \\ 0.0380 + 0.0069i & 0.3102 & 2.118 + 0.0001i \\ 0.0635 + 0.1672i & 2.118 - 0.0001i & 51.63 \end{pmatrix} \text{GeV}. \quad (5.8)$$

Noting that $F = fv_\xi = \text{diag}(f_1, f_2, f_3)v_\xi$ in eq. (5.5), $v_\xi = 10\,\text{MeV}$ gives $(f_1, f_2, f_3) = (0.0236, -0.38, 1.5)$. Then the allowed solution to RGEs for gauge coupling unification with $M_R^0 = v_R = 5\,\text{TeV}$ gives $M_{N_1} = 115\,\text{GeV}$, $M_{N_2} = -1.785\,\text{TeV}$, and $M_{N_3} = 7.5\,\text{TeV}$. While the first RH neutrino is lighter than the current experimental limit on Z_R boson mass, the second one is in-between the Z_R and W_R boson mass limits , but the heaviest one is larger than the W_R mass limit. These are expected to provide interesting collider signatures at LHC and future accelerators. Then following the top-down approach we obtain the value of M_D at the TeV scale

$$M_D(M_R^0) = \begin{pmatrix} 0.02274 & 0.0989 - 0.0160i & 0.1462 - 0.3859i \\ 0.0989 + 0.0160i & 0.6319 & 4.884 + 0.0003i \\ 0.1462 + 0.3859i & 4.884 - 0.0003i & 117.8 \end{pmatrix} \text{GeV}\,. \quad (5.9)$$

We will use $M_N = (0.115, -1.785, 7.5)\,\text{TeV}$ and the M_D matrix of eq. (5.9) to predict LFV and LNV decays in the next two sections.

6 Fitting the neutrino oscillation data by gauged inverse seesaw formula

In the presence of three singlet fermions S_i, $(i = 1, 2, 3)$, the inverse seesaw mechanism [39, 66–68, 71] is implemented in the present model through the SO(10) invariant Yukawa Lagrangian that gives rise to the G_{2113} invariant interaction near the TeV scale [39, 71] where $\chi_R(1, 1/2, -1, 1) \subset 16_H$ generates the $N - S$ mixing term,

$$\begin{aligned} \mathcal{L}_{\text{Yuk}} &= Y^a \mathbf{16.16}.10_H^a + f\mathbf{16.16}.126^\dagger{}_H + y_\chi \mathbf{16.1}.16^\dagger{}_H + \mu_{\mathbf{S}}\mathbf{1.1} \\ &\supset Y^\ell \overline{\ell}_L\, N_R\, \Phi_1 + f\, N_R^c\, N_R \Delta_R + F\, \overline{N}_R\, S\, \chi_R + S^T \mu_S S + \text{h.c.}. \end{aligned}$$

This Lagrangian gives rise to the 9×9 neutral fermion mass matrix after electroweak symmetry breaking.

$$\mathcal{M} = \begin{pmatrix} 0 & 0 & M_D \\ 0 & \mu_S & M \\ M_D^T & M^T & M_N \end{pmatrix}, \quad (6.1)$$

In contrast to the SM where all three matrices M_N, M, and μ_S have no dynamical origins, in this model the first two have dynamical interpretations $M_N = fv_R$, $M = y_\chi v_\chi$; only μ_S suffers from this difficulty.

In this model the RH neutrinos being heavier than the other two fermion mass scales in the theory with $M_N \gg M > M_D, \mu_S$, they are at first integrated out from the Lagrangian, which, in the $(\nu,\ S)$ basis, gives the 6×6 mass matrix

$$\mathcal{M}_{\text{eff}} = -\begin{pmatrix} M_D M_N^{-1} M_D^T & M_D M_N^{-1} M^T \\ M M_N^{-1} M_D^T & M M_N^{-1} M^T - \mu_S \end{pmatrix}, \quad (6.2)$$

JHEP01(2015)045

This is further block diagonalised to find that the would be dominant $type-I$ seesaw contribution completely cancels out leading to the gauged inverse mass formula for light neutrino mass matrix and also another formula for the sterile neutrinos(S)

$$m_\nu = M_D M^{-1} \mu_S (M_D M^{-1})^T \tag{6.3}$$

$$m_S = \mu_S - M M_N^{-1} M^T . \tag{6.4}$$

The complete 6×6 unitary mixing matrix which diagonalizes the light-sterile neutrino effective mass matrix $\mathcal{M}_{\rm eff}$ is

$$\begin{aligned}\mathcal{V}_{6\times 6} &= \mathcal{W}\cdot\mathcal{U} \\ &= \begin{pmatrix} 1-\frac{1}{2}XX^\dagger & X \\ -X^\dagger & 1-\frac{1}{2}X^\dagger X \end{pmatrix}\cdot\begin{pmatrix} U_\nu & 0 \\ 0 & U_S \end{pmatrix} .\end{aligned} \tag{6.5}$$

In this extended inverse seesaw scheme, the light neutrinos are actually diagonalized by a matrix which is a part of the full 6×6 mixing matrix $\mathcal{V}_{6\times 6}$

$$\mathcal{N} \simeq \left(1-\frac{1}{2}X\,X^\dagger\right) U_{\rm PMNS} = (1-\eta)\, U_{\rm PMNS} \tag{6.6}$$

where $\eta = \frac{1}{2} M_D M^{-1} (M_D M^{-1})^\dagger$ is a measure of non-unitarity contributions. In the (ν, S, N) basis, adding RH Majorana mass M_N to eq. (6.2), the complete mixing matrix [39, 73] diagonalizing the resulting 9×9 neutrino mass matrix turns out to be

$$\begin{aligned}\mathcal{V} &\equiv \begin{pmatrix} \mathcal{V}^{\nu\nu}_{\alpha i} & \mathcal{V}^{\nu S}_{\alpha j} & \mathcal{V}^{\nu N}_{\alpha k} \\ \mathcal{V}^{S\nu}_{\beta i} & \mathcal{V}^{SS}_{\beta j} & \mathcal{V}^{SN}_{\beta k} \\ \mathcal{V}^{N\nu}_{\gamma i} & \mathcal{V}^{NS}_{\gamma j} & \mathcal{V}^{NN}_{\gamma k} \end{pmatrix} \\ &= \begin{pmatrix} \left(1-\frac{1}{2}XX^\dagger\right)U_\nu & \left(X-\frac{1}{2}ZY^\dagger\right)U_S & Z\,U_N \\ -X^\dagger\,U_\nu & \left(1-\frac{1}{2}\{X^\dagger X+YY^\dagger\}\right)U_S & \left(Y-\frac{1}{2}X^\dagger Z\right)U_N \\ y^*\,X^\dagger\,U_\nu & -Y^\dagger\,U_S & \left(1-\frac{1}{2}Y^\dagger Y\right)\,U_N \end{pmatrix} ,\end{aligned} \tag{6.7}$$

where $X = M_D\,M^{-1}$, $Y = M\,M_N^{-1}$, $Z = M_D\,M_N^{-1}$, and $y = M^{-1}\,\mu_S$.

Although the $N-S$ mixing matrix M in general can be non diagonal, we have assumed it to be diagonal partly to reduce the unknown parameters and as we shall see the LFV effects constrain the diagonal elements. Noting that $\eta_{\alpha\beta} = \frac{1}{2}\sum_{k=1}^{3}(M_{D_{\alpha k}}\,M^*_{D_{\beta k}})/M_k^2$, the entries of the η matrix are constrained from various experimental inputs like e.g. rare leptonic decays, invisible Z-boson width, neutrino oscillations etc. For illustration let us quote the bound on these elements of η on 90% C.L.[3] $|\eta_{ee}| \leq 2.0\times 10^{-3}$, $|\eta_{\mu\mu}| \leq 8.0\times 10^{-4}$, $|\eta_{\tau\tau}| \leq 2.7\times 10^{-3}$, $|\eta_{e\mu}| \leq 3.5\times 10^{-5}$, $|\eta_{e\tau}| \leq 8.0\times 10^{-3}$, and $|\eta_{\mu\tau}| \leq 5.1\times 10^{-3}$. Whereas the possible CP phases of the elements of $\eta_{\alpha\beta}$ $(=\phi_{\alpha\beta})$ are not constrained, the knowledge of M_D matrix given in eq. (5.9) and saturation of the lower bound on $|\eta_{\tau\tau}| = 2.7\times 10^{-3}$ leads to a relation between diagonal elements of M,

$$\frac{1}{2}\left[\frac{\kappa_1}{M_1^2}+\frac{\kappa_2}{M_2^2}+\frac{\kappa_3}{M_3^2}\right] = 2.7\times 10^{-3} , \tag{6.8}$$

[3]For related references on the 90% C.L of the bounds on the elements $|\eta_{\alpha\beta}|$ see references cited in [39, 71].

JHEP01(2015)045

where

$$\kappa_1 = 0.17\,\mathrm{GeV}^2, \quad \kappa_2 = 23.853\,\mathrm{GeV}^2, \quad \kappa_3 = 13876.84\,\mathrm{GeV}^2\,. \tag{6.9}$$

The above relation can be satisfied by the partial degenerate values of M as $M_1 = M_2 \geq 100\,\mathrm{GeV}$ and $M_3 \geq 2.15\,\mathrm{TeV}$ while it also accommodates the complete non-degenerate values $M_1 \geq 10\,\mathrm{GeV}$, $M_2 \geq 120\,\mathrm{GeV}$, and $M_3 \geq 2.6\,\mathrm{TeV}$. For degenerate M, this gives $M_1 = M_2 = M_3 = 1.6\,\mathrm{TeV}$. The elements of η can be different for different values of M allowed in our model. We need to know the PMNS mixing matrix and η in order to estimate the non-unitarity leptonic mixing matrix $\mathcal{N}_{3\times3}$.

Our analysis carried out for a normal hierarchy (NH) of light neutrino masses can be repeated also for inverted hierarchical (IH) or for quasi-degenerate (QD) masses to give correspondingly different values of the μ_S matrix. For example, using NH for which $\hat{m}_\nu^{\rm diag} = \mathrm{diag}(0.00127\ ,\ 0.00885\ ,\ 0.0495\ )\,\mathrm{eV}$ consistent with the central values of a recent global analysis of the neutrino oscillation parameters [74–76] $\Delta m^2_{\rm sol} = 7.62\times10^{-5}\,\mathrm{eV}^2$, $\Delta m^2_{\rm atm} = 2.55\times10^{-3}\,\mathrm{eV}^2$, $\theta_{12} = 34.4^\circ$, $\theta_{23} = 40.8^\circ, \theta_{13} = 9.0^\circ, \delta = 0.8\pi$ and assuming vanishing Majorana phases $\alpha_1 = \alpha_2 = 0$, we use the non-unitarity mixing matrix $\mathcal{N} = (1-\eta)\,U_{\rm PMNS}$, and the relation $m_\nu = \mathcal{N}\hat{m}_\nu\mathcal{N}^T$, to derive the form of μ_S matrix from the light neutrino mass formula (6.3)

$$\begin{aligned}\mu_S &= X^{-1}\,\mathcal{N}\hat{m}_\nu\mathcal{N}^T\,(X^T)^{-1}\\ &= \begin{pmatrix} 0.001+0.0004\,i & -0.0026-0.0012\,i & 0.0013\\ -0.0026-0.0012\,i & 0.0067+0.0023\,i & -0.0034\\ 0.0013 & -0.0034 & 0.0014-0.0006\,i\end{pmatrix}\mathrm{GeV}\,.\end{aligned} \tag{6.10}$$

7 Lepton flavor violations

Within the framework of this extended seesaw scheme [39], the dominant contributions are mainly through the exchange of heavy sterile neutrinos (S) as well as heavy RH neutrinos (N_R) with branching ratio [39, 71, 77–80]

$$\mathrm{Br}\,(\ell_\alpha \to \ell_\beta + \gamma) = \frac{\alpha_{\rm w}^3\, s_{\rm w}^2\, m_{\ell_\alpha}^5}{256\,\pi^2\, M_W^4\,\Gamma_\alpha}\left|\mathcal{G}^N_{\alpha\beta} + \mathcal{G}^S_{\alpha\beta}\right|^2\,, \tag{7.1}$$

$$\text{where } \mathcal{G}^N_{\alpha\beta} = \sum_k \left(\mathcal{V}^{\nu\,N}\right)_{\alpha\,k}\left(\mathcal{V}^{\nu\,N}\right)^*_{\beta\,k}\mathcal{F}\left(\frac{m^2_{N_k}}{M^2_{W_L}}\right),$$

$$\mathcal{G}^S_{\alpha\beta} = \sum_j \left(\mathcal{V}^{\nu S}\right)_{\alpha\,j}\left(\mathcal{V}^{\nu S}\right)^*_{\beta\,j}\mathcal{F}\left(\frac{m^2_{S_j}}{M^2_{W_L}}\right),$$

$$\text{with } \mathcal{F}(x) = -\frac{2x^3+5x^2-x}{4(1-x)^3} - \frac{3x^3\ln x}{2(1-x)^4}\,.$$

Here the summation over j and k goes over number of sterile neutrinos S_j and for heavy right-handed Majorana neutrinos N_k and the mixing matrices are $\mathcal{V}^{\nu S}_{\alpha\,j} = \{X\,U_S\}_{\alpha\,j}$ and $\mathcal{V}^{\nu N}_{\alpha\,k} = \{Z\,U_N\}_{\alpha\,k}$ with $X = \frac{M_D}{M}$ and $Z = \frac{M_D}{M_N}$. The allowed ranges of $M_i, (i = 1, 2, 3)$ from

JHEP01(2015)045

the LFV constraint eq. (6.8) and the predicted values of $M_{N_i}, (i = 1, 2, 3)$ now determine the mass eigenvalues of the sterile neutrinos leading to $M_{S_i} = \{12.5, 49, 345.6\}$ GeV for $M = \text{diag}[40, 300, 1661]$ GeV, and $M_N = \text{diag}[115, -1785, 7500]$ GeV.

The neutrino mixing matrices are estimated numerically

$$\mathcal{N} \equiv \mathcal{V}^{\nu\nu} = \begin{pmatrix} 0.8143 - 0.0008i & 0.5588 + 0.0002i & 0.1270 + 0.0924i \\ -0.3587 - 0.0501i & 0.6699 - 0.0343i & -0.6472 - 0.0001i \\ 0.4489 - 0.0571i & -0.4849 - 0.0394 & -0.7438 - 0.0001i \end{pmatrix}, \tag{7.2}$$

$$\mathcal{V}^{\nu S} = \begin{pmatrix} 0.0542 & 0.0325 - 0.0052i & 0.0086 - 0.0227i \\ 0.2358 + 0.0380i & 0.2075 & 0.2869 \\ 0.3465 + 0.9159i & 1.597 & 6.920 \end{pmatrix} \times 10^{-2} i\,, \tag{7.3}$$

$$\mathcal{V}^{\nu N} = \begin{pmatrix} 0.0170 & 0.0053 - 0.0009i & 0.0018 - 0.0048i \\ 0.0740 + 0.0119i & 0.0340 & 0.0608 \\ 0.1089 + 0.2865i & 0.2625 & 1.467 \end{pmatrix} \times 10^{-2}\,. \tag{7.4}$$

Compared to RH neutrinos, the branching ratios due to exchanges of sterile neutrino (S_i) are found to be more dominant

$$\text{Br}\,(\mu \to e + \gamma) = 3.5 \times 10^{-16}. \tag{7.5}$$

Similarly, other LFV decay amplitudes are estimated leading to [81]

$$\begin{aligned} \text{Br}\,(\tau \to e + \gamma) &= 3.0 \times 10^{-14}\,, \\ \text{Br}\,(\tau \to \mu + \gamma) &= 4.1 \times 10^{-12}\,. \end{aligned} \tag{7.6}$$

These branching ratios are accessible to ongoing search experiments

We have also noted here that the leptonic CP-violating parameter due to non-unitarity effects is $J \simeq 10^{-5}$ which is similar to the model prediction of ref. [39].

8 New contributions to neutrino-less double beta decay in the $W_L - W_L$ channel

8.1 Sterile neutrino mass from effective mass

In the generic inverse seesaw, there is only one small lepton number violating scale μ_S and the lepton number is conserved in the $\mu_S = 0$ limit leading to vanishing non-standard contribution to the $0\nu2\beta$ transition amplitude. On the contrary, in the extended seesaw under consideration, it has been shown for the first time that there can be a new dominant contributions from the exchanges of heavy sterile neutrinos [39]. The main thrust of our discussion will be new contribution arising from exchange of heavy sterile neutrinos S_i with Majorana mass $M_S = \mu_S - M(1/M_N)M^T$ as explained in section 6 when added to the light neutrino exchange contribution with different mass hierarchies, NH, IH, and QD patterns. Although dominance of sterile neutrino exchange was estimated very approximately in ref. [39], its interference with light neutrino contribution was neglected. Also no bound on the lightest sterile neutrino mass or an analytic expression for half life as discussed here

JHEP01(2015)045

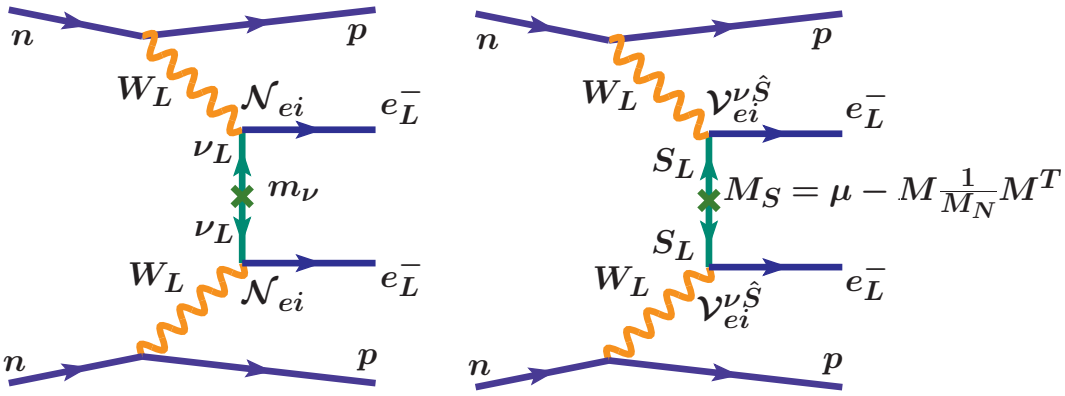

Figure 6. Feynman diagrams for $0\nu\beta\beta$ decay in the $W_L^- - W_L^-$ channel with light ν_i exchange (left-panel) and sterile S_i Majorana neutrino exchange (right-panel).

was possible in that work. Other high-light of the present analysis is our new scattered plot of effective mass parameter against the lightest active neutrino mass in the theory, plot of combined effective mass parameter against lightest sterile neutrino mass, scattered plots of half life against lightest sterile neutrino mass and functional plot of half life against lightest sterile neutrino mass in different cases. Because of heavy mass of W_R boson in this theory, the RH current contributions are damped out.

In the mass basis, we have $\nu_\alpha = \mathcal{N}_{\alpha\, i}\, \nu_{m_i} + \mathcal{V}_{\alpha\, j}^{\nu S}\, S_{m_j}$. In addition to the well known standard contribution in the $W_L^- - W_L^-$ channel shown in the left-panel of figure 6, the new contribution is shown in the right-panel of figure 6 with the corresponding amplitudes

$$\mathcal{A}_\nu^{LL} \propto G_F^2 \frac{(\mathcal{V}_{e\, i}^{\nu\nu})^2\, m_{\nu_i}}{p^2}\,, \tag{8.1}$$

$$\mathcal{A}_S^{LL} \propto G_F^2 \frac{\left(\mathcal{V}_{e\, j}^{\nu S}\right)^2}{M_{S_j}}\,. \tag{8.2}$$

where $|p^2|$ represents magnitude square of neutrino virtuality momentum and $G_F = 1.2 \times 10^{-5}\,\mathrm{GeV}^{-2}$.

The analytic expression for the amplitude due to RH neutrino exchange is similar to the singlet fermion exchange but with the replacement $\mathcal{V}_{e\, j}^{\nu S} \to \mathcal{V}_{e\, j}^{\nu N}$ and $M_{S_j} \to M_{N_j}$ in the second equation given above. As the RH neutrinos are necessarily heavier than the sterile fermion masses because of the underlying constraint imposed by the extended see-saw mechanism, we ignore their contribution and consider the combined effective mass parameter due to two sources: the light neutrino and the sterile fermion exchanges in the $W_L - W_L$ channel.

$$\begin{aligned} m_{ee}^{\mathrm{eff}} &= m_{ee}^{\nu} + m_{ee}^{\mathrm{S}}, \\ m_{\mathrm{ee}}^{\nu} &= \mathcal{N}_{e\,1}^2 m_{\nu_1} + \mathcal{N}_{e\,2}^2 m_{\nu_2} e^{2i\alpha_1} + \mathcal{N}_{e\,3}^2 m_{\nu_3} e^{2i\alpha_2}\,, \end{aligned} \tag{8.3}$$

$$m_{\mathrm{ee}}^{S} = p^2 \sum_i \frac{\left(\mathcal{V}_{e\, i}^{\nu S}\right)^2}{\hat{M}_{S_i}}\,, \tag{8.4}$$

JHEP01(2015)045

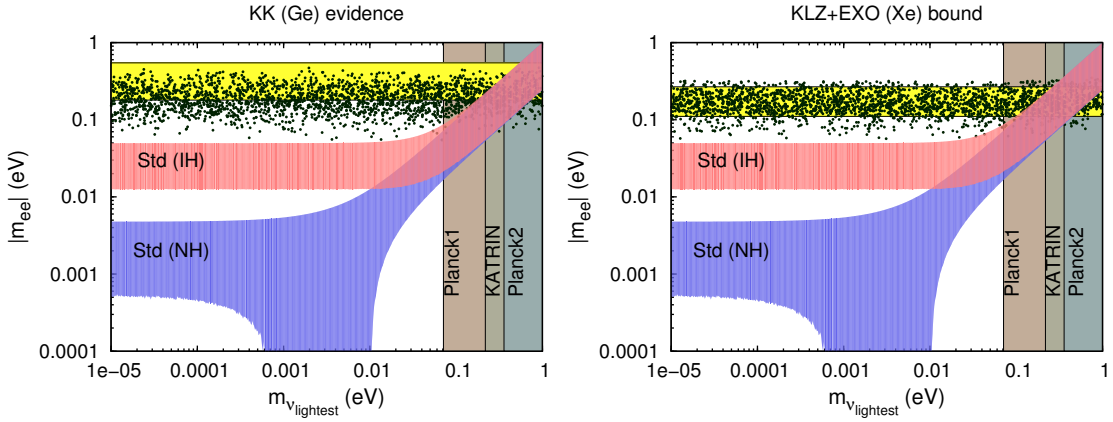

Figure 7. Effective mass as a function of the lightest active neutrino mass. The blue and the red bands correspond to normal and inverted hierarchy, respectively. The vertical bands are from the bounds on the sum of light neutrino masses given by Planck1, Planck2, and KATRIN experiments. The horizontal yellow band in the left panel corresponds to HM claim with $T^{0\nu}_{1/2}(^{76}\text{Ge}) = 2.23^{+0.44}_{-0.31} \times 10^{25}$ yrs at 68% C.L. and that in the right-panel corresponds to the KamLAND-Zen and EXO-200 combined bound $T^{0\nu}_{1/2}(^{136}\text{Xe}) = 3.4 \times 10^{25}$ yrs at 90% C.L. The scattered points are sterile neutrino contributions to the effective mass.

where, in the second equation, we have introduced two Majorana phases, α_1, α_2, in the light neutrino mixing matrix. Noting from eq. (6.7) that $(\mathcal{V}^{\nu S}_{ej})^2 = (M_D/M)^2_{ej}$, the r.h.s. of eq. (8.4) is expected to dominate because of three reasons:(i) Dirac neutrino mass origin from quark-lepton symmetry in SO(10), (ii) Smaller values of diagonal elements of the $N - S$ mixing matrix M, (iii) smaller eigenvalues of the heavy sterile Majorana neutrino mass: $M_S = \mu_S - M(1/M_N)M^T$. The mixing matrix elements necessary for prediction of $0\nu\beta\beta$ amplitude can be extracted from eq. (7.2) and eq. (7.3) as,

$$\begin{aligned} &\mathcal{N}_{e1} = 0.8143 - 0.0008i, \quad \mathcal{N}_{e2} = 0.5588 + 0.0002i, \quad \mathcal{N}_{e3} = 0.1270 + 0.0924i\,, \\ &\mathcal{V}^{\nu S}_{e1} = 0.00054i, \quad \mathcal{V}^{\nu S}_{e2} = 0.00005 + 0.00032i, \quad \mathcal{V}^{\nu S}_{e3} = 0.00023 + 0.00009i\,. \end{aligned} \tag{8.5}$$

In figure 7 we have presented the effective mass parameter for $0\nu\beta\beta$ decay as a function of lightest neutrino mass. The yellow band in the left-panel represents the Heidelberg-Moscow (HM) evidence corresponding to measured half-life $T^{0\nu}_{1/2}(^{76}\text{Ge}) = 2.23^{+0.44}_{-0.31} \times 10^{25}$ yrs at 68% C.L. In the right-panel it represents the combined bound from KamLAND-Zen and EXO-200 experiments corresponding to $T^{0\nu}_{1/2}(^{136}\text{Xe}) = 3.4 \times 10^{25}$ yrs at 90% C.L. The effective mass predictions for normal and inverted hierarchy of light neutrinos which are known to be far below the current experimental bounds are also shown in the left- and the right- panels. In both these panels the quasi-degenerate mass region is shown by vertical lines to the right of each figure and the corresponding contributions to the effective mass is shown by the slanting band of the hammer shaped region.

In order to obtain the scattered dots in this figure at first we have used dominance of sterile neutrino exchange. The combined effect of light and sterile neutrino exchanges are discussed in subsequent figures. The nuclear matrix elements and phase space factors are taken from the table 4. The diagonal elements of M have been obtained from non-

JHEP01(2015)045

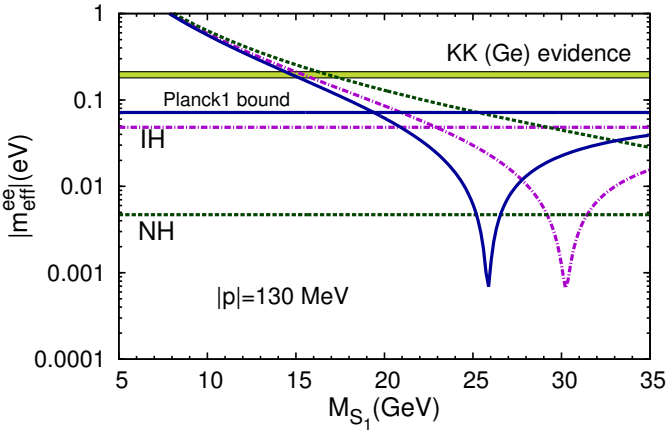

Figure 8. Effective mass as a function of lightest sterile neutrino mass. The green band corresponds to the effective mass corresponding to HM experiment. Horizontal lines are the standard effective masses in the NH, IH, and saturation of Planck1 pattern of light neutrino masses in the absence of any Majorana phase. The solid, dashed, and the dotted curves are for ligt-neutrino masses corresponding to saturation of Planck1 bound, IH, and NH patterns. We have used $\langle p^2 \rangle = (130\,\text{MeV})^2$.

unitarity constraint discussed in section 6 and the specific values are $M_1 = 55\,\text{GeV}$, $M_2 \in [250, 550]$, and $M_3 \in [1600, 2500]\,\text{GeV}$. Including the estimated matrices M_D and M_N already discussed, we get $M_{S1} \simeq 22\,\text{GeV}$ and much larger values of M_{S2}, M_{S3} to generate these scattered dots. For values of M_{S_1} smaller (larger) than 22 GeV, the central region of the scattered points is noted to shift upwards (downwards). Thus, we find that even without the quasi-degeneracy assumption on the light neutrino masses, it is possible to explain the current experimental bounds or any future data close to these limits by the sterile neutrino dominance.

As the standard and sterile contributions to effective mass parameter have opposite signs, there is the possibility of cancellation between the two terms if Majorana phases are neglected. This behavior of the combined contribution is depicted in figure 8.

Saturation of the Plank1 bound on the sum of the three light neutrino masses at 0.23 eV [13] combined with neutrino oscillation data gives $(\hat{m}_1, \hat{m}_2, \hat{m}_3) = (0.0712, 0.0717, 0.0870)\,\text{eV}$, or $(\hat{m}_1, \hat{m}_2, \hat{m}_3) = (0.0820, 0.0824, 0.0655)\,\text{eV}$. Contribution of such light neutrinos alone to the effective mass which is shown by the solid-blue horizontal line is way below the HM data or the combined bound from KamLAND-Zen and EXO-200 experiments. The light neutrino contributions of IH and NH type are shown by the dashed-magenta and the dotted-green horizontal lines in this figure whereas the combined effective mass parameters including sterile neutrino contributions are represented by the corresponding slanting curves. A dip in the solid-blue curve that includes contribution of light neutrino masses of Planck1 type hierarchy occurs at $\hat{M}_{S_1} \simeq 26\,\text{GeV}$, but the corresponding dip in the dotted-magenta curve that includes contribution of IH type neutrinos is found to occur at $\hat{M}_{S_1} \simeq 30\,\text{GeV}$. We have also noted that the cancellation between the light neutrino and sterile neutrino contributions occurs at still larger value of

JHEP01(2015)045

$\hat{M}_{S_1} \geq 40\,\text{GeV}$. This cancellation phenomenon with increasing values of dip positions for decreasing values of light neutrino masses as evidenced in Planck1, IH, and NH cases is clearly understood by our formulas given in eq. (8.3) and by noting that all sterile neutrino mass eigenvalues $\hat{M}_{S_i}$ are negative. Being inversely proportional to $\hat{M}_{S_i}$, the sterile neutrino contribution decreases for increasing mass eigenvalues and the dip region appears when the sterile neutrino contribution is comparable to the naturally small contribution due to the light neutrinos of a given type of hierarchy.

We also note the occurrence of a stringent bound on the mass of the lightest sterile neutrino $\hat{M}_{S_1} \geq 15\,\text{GeV}$ from the crossing region of the HM experimental band. This smallest value occurs for smallest allowed value of $|p| = 130\,\text{MeV}$ and large values of $(\hat{M}_{S_2}, \hat{M}_{S_3}) = (160, 758)\,\text{GeV}$ so that the contributions of the latter two masses are negligible. For larger values of $|p|$, the bound on M_{S_1} will be larger. We will discuss this issue later in this section in the context of half-life predictions for $0\nu\beta\beta$-decay where peaks are expected to appear.

The cancellation among the light neutrino and sterile neutrino contributions is more prominent in the quasi-degenerate case as shown in figure 9 where the horizontal overlapping dark region shows that, in the absence of both the Majorana phases, the contribution of light quasi-degenerate neutrinos alone with common mass $m_\nu = 0.23\,\text{eV}$ can explain the HM data with nuclear matrix element $M^\nu_{0\nu} = 6.64$. On the other hand, in the presence of sterile neutrinos, the two contributions cancel out for certain allowed values of parameters giving much smaller value of the resultant effective mass for certain values of $\hat{M}_{S_1}$. In the figure 9, the first dip in the effective mass occurs at $\hat{M}_{S_1} \simeq 15.8\,\text{GeV}$ for zero Majorana phases of light-neutrinos. This behavior is shown by the solid-blue curve. The dip in the region $M_{S_1} \simeq 25\,\text{GeV}$ occurs when each of the two Majorana phases in the light neutrino sector is $\pi/2$. The orange band shown in the figure 9 spans over all the possible values of the two Majorana phases between $0 - 2\pi$. We have shown one case by the dot-dashed green curve which corresponds to Majorana phase $\alpha_1 = \pi/4$. We have noted that for larger values of $|p|$, the cancellation and the dip regions shift towards higher values of $\hat{M}_{S_1}$.

From the figure 8 and the figure 9 it is clear that for agreement with the current experimental data on the effective mass parameter, the lightest sterile neutrino mass should be constrained with the following lower bonds

$$\begin{aligned} \hat{M}_{S_1} &\geq 11.7\,\text{GeV},\ \text{QD}, \\ &\geq 14.5\,\text{GeV},\ \text{Plank1}, \\ &\geq 14.5\,\text{GeV},\ \text{IH}, \\ &\geq 16.3\,\text{GeV},\ \text{NH}. \end{aligned} \tag{8.6}$$

8.2 A formula for half-life and bound on sterile neutrino mass

We derive a new formula for half-life of $0\nu\beta\beta$ decay as a function of heavy sterile neutrino masses and other parameters in the theory. We then show by means of scattered plots or otherwise, how the current experimental bounds limit the lightest sterile neutrino mass.

JHEP01(2015)045

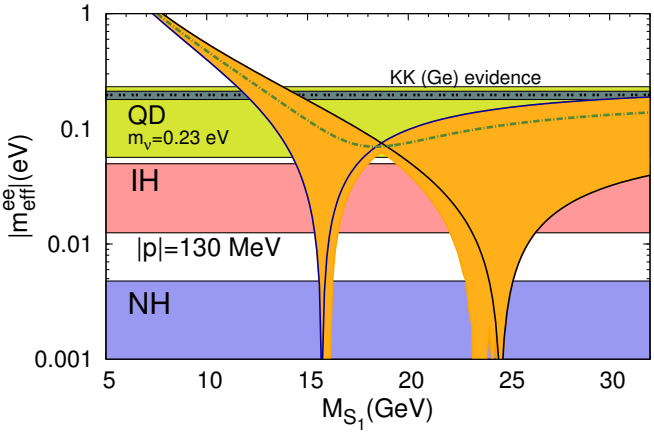

Figure 9. Predicted variation of combined effective mass parameter for $0\nu\beta\beta$ decay as a function of lightest sterile neutrino mass $\hat{M}_{S_1}$. The horizontal blue, red and green bands of effective masses are generated for the NH, IH, and the QD type of light neutrinos, respectively when all the Majorana phases are scanned. The yellow band represents the HM data. The orange band is quasi-degenerate light + sterile neutrino contribution for fixed $\mathcal{M}^{\nu}_{0\nu} = 6.64$ and $|p| = 130\,\text{MeV}$.

Isotope	$G^{0\nu}_{01}[10^{-14}\text{yrs}^{-1}]$ refs. [39, 82]	$\mathcal{M}^{0\nu}_{\nu}$	$\mathcal{M}^{0\nu}_{N}$
^{76}Ge	0.686	2.58–6.64	233–412
^{82}Se	2.95	2.42–5.92	226–408
^{130}Te	4.13	2.43–5.04	234–384
^{136}Xe	4.24	1.57–3.85	160–172

Table 4. Phase space factors and nuclear matrix elements with their allowed ranges as derived in refs. [39, 82–84].

Using results discussed in previous sections, the inverse half-life is presented in terms of $\eta-$ parameters and others including the nuclear matrix elements [39, 82–84]

$$\left[T^{0\nu}_{1/2}\right]^{-1} = G^{0\nu}_{01}|\mathcal{M}^{0\nu}_{\nu}|^2|\eta_{\nu} + \frac{\mathcal{M}^{0\nu}_{N}}{\mathcal{M}^{0\nu}_{\nu}}\eta_S|^2\,, \tag{8.7}$$

where the dimensionless particle physics parameters are

$$\eta_{\nu} = \sum_i \frac{(\mathcal{V}^{\nu\nu}_{ei})^2\, m_i}{m_e}, \qquad \eta_S = \sum_i \frac{(\mathcal{V}^{\nu S}_{ei})^2\, m_p}{M_{S_i}}\,. \tag{8.8}$$

In eq. (8.8), m_e (m_i)= mass of electron (light neutrino), and m_p = proton mass. In eq. (8.7), $G^{0\nu}_{01}$ is the the phase space factor and, besides different particle parameters, it contains the nuclear matrix elements due to different chiralities of the hadronic weak currents such as $\mathcal{M}^{0\nu}_{\nu}$ involving left-left chirality in the standard contribution. Explicit numerical values of these nuclear matrix elements discussed in refs. [39, 82–84] are given in table 4.

JHEP01(2015)045

In terms of effective mass parameter, the inverse half-life for $0\nu\beta\beta$ decay is

$$\begin{aligned}\left[T^{0\nu}_{1/2}\right]^{-1} &= \frac{\Gamma_{0\nu\beta\beta}}{\ln 2} = G_{0\nu}\left|\frac{\mathcal{M}^{0\nu}_{\nu}}{m_e}\right|^2 \times |m^{\rm eff}_{ee}|^2\,, \\ m^{\rm eff}_{ee} &= m^{\nu}_{ee} + m^{\rm S}_{ee}\,,\end{aligned} \tag{8.9}$$

where $G_{0\nu}$ contains the phase space factors, m_e is the electron mass, and $\mathcal{M}_\nu$ is the nuclear matrix element and the effective mass parameters are

$$m^{\nu}_{\rm ee} = \mathcal{N}^2_{e\,i} m_{\nu_i}\,, \quad m^{S}_{\rm ee} = p^2\,\frac{\left(\mathcal{V}^{\nu S}_{e\,i}\right)^2}{\hat{M}_{S_i}}\,, \tag{8.10}$$

where $p^2 = -|p^2|$ and

$$\begin{aligned}\left|\langle p^2\rangle\right| &= \left|m_e m_p \mathcal{M}^{0\nu}_{N}/\mathcal{M}^{0\nu}_{\nu}\right| \\ &= [(130-277)\ \text{MeV}]^2\,, \quad {}^{76}\text{Ge}, \\ &= [(140-230)\ \text{MeV}]^2\,, \quad {}^{136}\text{Xe}\,.\end{aligned} \tag{8.11}$$

Neglecting Majorana phases, the numerical estimation for light neutrino contribution for the effective mass is

$$\begin{aligned}|m^{\nu}_{\rm ee}| &= \mathcal{N}^2_{e\,1}\, m_{\nu_1} + \mathcal{N}^2_{e\,2}\, m_{\nu_2} + \mathcal{N}^2_{e\,3}\, m_{\nu_3} \\ &\simeq 0.004\,\text{eV} \quad \text{NH}, \\ &\simeq 0.048\,\text{eV} \quad \text{IH}, \\ &\simeq 0.23\,\text{eV} \quad \text{QD}.\end{aligned} \tag{8.12}$$

For direct prediction of half-life as a function of heavy sterile neutrino masses and its comparison with experimental data of ongoing search experiments, we derive the following analytic formula including light neutrino contribution

$$T^{0\nu}_{1/2} = \mathcal{K}^{-1}_{0\nu} \times \frac{M^2_{N_1} M^4_{S_1}}{|\langle p^2\rangle|^2\,(M_{D_{e1}})^4}\left[\left|1 + \mathbf{a}\frac{M^2_{S_1}}{M^2_{S_2}} + \mathbf{b}\frac{M^2_{S_1}}{M^2_{S_3}} - \boldsymbol{\delta}\right|\right]^{-2}, \tag{8.13}$$

where $K_{0\nu} = G_{0\nu}\left|\frac{\mathcal{M}^{0\nu}_{\nu}}{m_e}\right|^2 \sim \mathcal{O}(10^{-25})\ \text{yrs}^{-1}\ \text{eV}^{-2}$ and

$$\mathbf{a} = \frac{M^2_{De2}}{M^2_{De1}}\frac{M_{N_1}}{M_{N_2}}\,, \qquad \mathbf{b} = \frac{M^2_{De3}}{M^2_{De1}}\frac{M_{N_1}}{M_{N_3}}\,, \qquad \boldsymbol{\delta} = \frac{m^{\nu}_{ee} M_{N_1}}{M^2_{De1}}\frac{M^2_{S_1}}{|p^2|}. \tag{8.14}$$

The light-neutrino contribution has entered through the quantity δ in the eq. (8.13). This formula is different from the one obtained using type-II seesaw dominance in SO(10) with TeV scale Z' [114] but a lower bound on the lightest sterile neutrino mass nearly one order smaller than those reported here. Further Type-II seesaw dominated SO(10) model has been utilised in ref. [114] with negligible $n-\bar{n}$ oscillation and rare-kaon decay amplitudes.

Using the predicted value of M_D from eq. (5.9) and derived values of heavy RH Majorana neutrino mass matrix, $M_N = \text{diag}(115, -1785, 7500)\,\text{GeV}$ from the GUT-scale fit to the fermion masses we obtain from eq. (8.14)

$$\mathbf{a} = -1.187 + i\,0.395\,, \qquad \mathbf{b} = -3.782 - i\,3.346. \tag{8.15}$$

JHEP01(2015)045

M (GeV)	$\lvert\hat{M}_S\rvert$ (GeV)[eq. (8.16)]	$\hat{M}_{S_{\rm exact}}$ (GeV) [NH]
(20, 550, 2500)	(3.48, 169, 833)	(3.38, 156, 758)
(25, 550, 2500)	(5.43, 169, 833)	(5.20, 156, 758)
(30, 550, 2500)	(7.82, 169, 833)	(7.35, 156, 758)
(35, 550, 2500)	(10.6, 169, 833)	(9.81, 156, 758)
(40, 550, 2500)	(13.9, 169, 833)	(12.5, 156, 758)
(45, 550, 2500)	(17.6, 169, 833)	(15.5, 156, 758)
(50, 550, 2500)	(21.7, 169, 833)	(18.7, 156, 758)
(55, 550, 2500)	(26.3, 169, 833)	(22.1, 156, 758)
(60, 550, 2500)	(31.3, 169, 833)	(25.6, 156, 758)
(65, 550, 2500)	(36.7, 169, 833)	(29.3, 156, 758)
(70, 550, 2500)	(42.6, 169, 833)	(33.1, 156, 758)
(75, 550, 2500)	(48.9, 169, 833)	(37.0, 156, 758)

Table 5. Eigenvalues of sterile neutrino mass matrix for different allowed $N - S$ mixing matrix elements.

For different values of the diagonal matrix $M = \text{diag}(\hat{M}_1, \hat{M}_2, \hat{M}_3)$ consistent with the non-unitarity constraint eq. (6.8), and the $M_N = \text{diag}(115, -1785, 7500)\,\text{GeV}$, we derive mass eigenvalues $\hat{M}_S = (\hat{M}_{S_1}, \hat{M}_{S_2}, \hat{M}_{S_3})$ using the formula

$$\hat{M}_S = -(M_1^2/M_{N_1}, M_2^2/M_{N_2}, M_3^2/M_{N_3}). \tag{8.16}$$

Alternatively, we have determined the mass eigenvalues $\hat{M}_{S_i}$ by direct diagonalization of the 9×9 neutral fermion mass matrix under the constraints from neutrino oscillation data and the extended seesaw. The moduli of these eigenvalues and the corresponding elements of M are given in table 5 where the values derived using eq. (8.16) have been denoted as $\hat{M}_S$, but those obtained by direct diagonalization of 9×9 matrix are denoted as $M_{S_{\rm exact}}$. It is clear from eq. (8.13) that the half-life is a function of three mass eigenvalues M_{S_1}, M_{S_2} and M_{S_3} while all other parameters are known. This calls for a scattered plot for half life as discussed below. It is evident from eq. (8.13) that for $M_{S_3} \gg M_{S_2} \gg M_{S_1}$, a $\log(T_{1/2})$ vs $\log(M_{S_1})$ would exhibit a linear behavior.

Including the contribution of light neutrinos with NH patterns of masses, we have shown the scattered plot of half-life as a function of lightest sterile neutrino mass M_{S_1} and compared it with experimental data from ^{76}Ge (left-panel) and ^{136}Xe (right panel) as shown in figure 10. Including the the contribution of light neutrinos with IH patterns of masses, the scattered plots are shown in the left-panel and the right panel of figure 11. Including contributions of light neutrinos with QD pattern of masses, the scattered plots for half life are shown in figure 12.

Compared to scattered plots of half-life in NH and IH cases, we find the spread in the dots is over a much wider region for $M_{S_1} > 15\,\text{GeV}$ in the QD case. This may be due to

JHEP01(2015)045

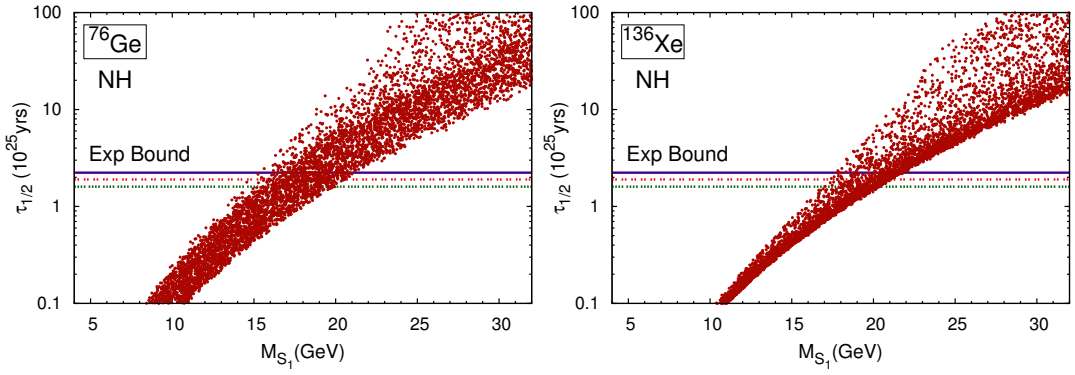

Figure 10. Scattered plot of half-life due to NH type light neutrino and heavy sterile neutrino exchange contributions in the $W_L - W_L$ channel as a function of lightest sterile mass. Left (right) panel corresponds to the nuclear matrix elements and phase space factor of ^{76}Ge (^{136}Xe). Details of various parameters is given in the text. The solid horizontal lines indicate the HM evidence.

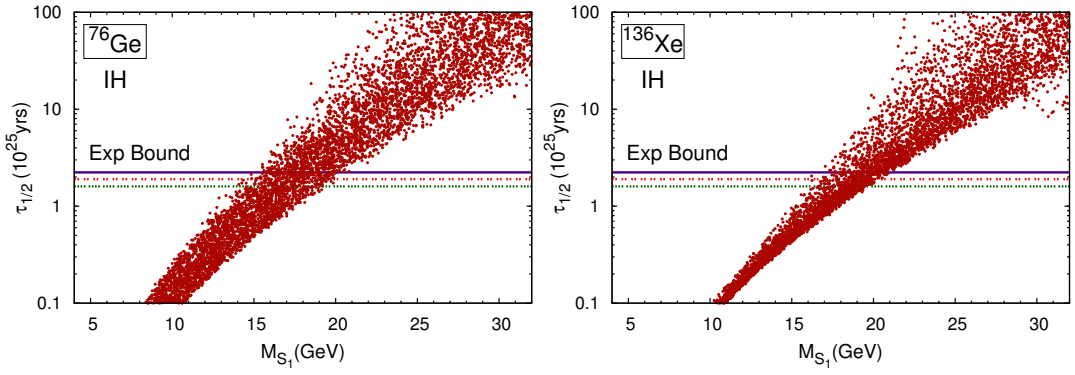

Figure 11. Same as figure 10 but for inverted hierarchy of light neutrino masses.

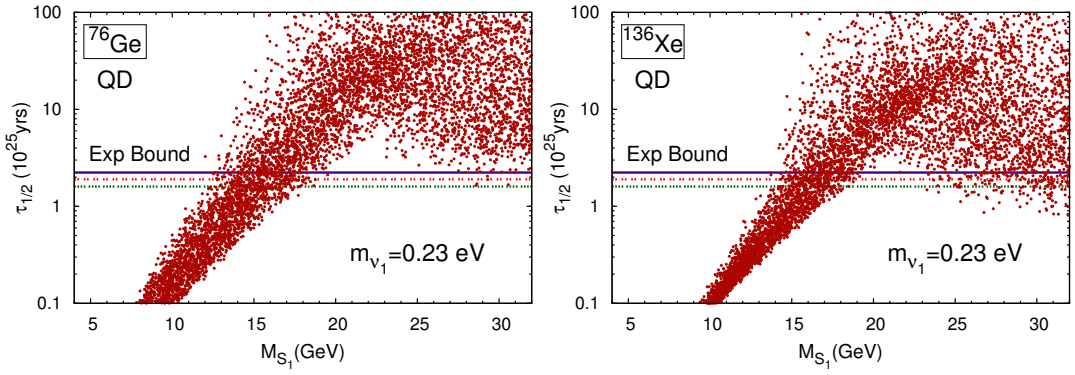

Figure 12. Same as figure 10 and figure 11 but for quasi-degenerate light neutrino masses with $m_\nu = 0.23\,\text{eV}$.

JHEP01(2015)045

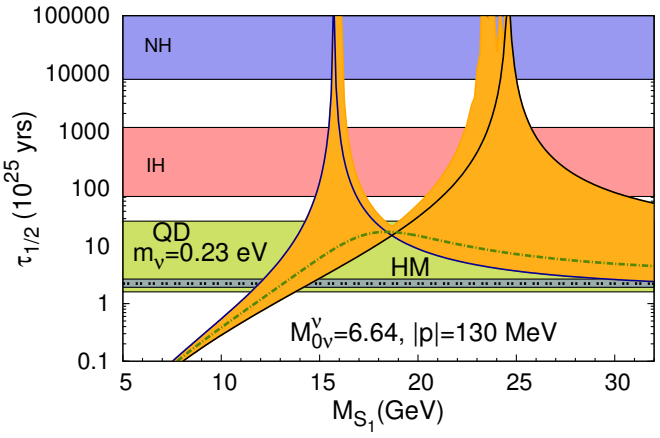

Figure 13. Predicted variation of half-life as a function of lightest sterile neutrino mass M_{S1}. The blue, red and green bands have been generated taking the normal, inverted and quasi-degenerate patterns of light neutrino masses, respectively when all the Majorana phases are scanned and sterile neutrino contributions are switched off. The orange band is the combined contribution with fixed nuclear matrix element, $\mathcal{M}^{\nu}_{0\nu} = 6.64$ and $|p| = 130\,\mathrm{MeV}$.

cancellation between the light neutrino and the sterile neutrino contributions. To analyse this aspect more vividly we have plotted the half-life as a function of $\hat{M}_{S_1}$ using eq. (8.13) and table 5 as shown in figure 13.

From the figure 10, figure 11, and figure 12, it is clear that the ^{76}Ge data gives the following bounds on the lightest sterile neutrino mass,

$$\begin{aligned} \hat{M}_{S_1} &\geq 15.5 \pm 3.5 \text{ GeV, QD,} \\ &\geq 18.0 \pm 3.0 \text{ GeV, IH,} \\ &\geq 18.5 \pm 3.0 \text{ GeV, NH.} \end{aligned} \tag{8.17}$$

whereas from the ^{136}Xe data, the bounds are

$$\begin{aligned} \hat{M}_{S_1} &\geq 17.0 \pm 3.0 \text{ GeV, QD,} \\ &\geq 19.0 \pm 2.0 \text{ GeV, IH,} \\ &\geq 20.0 \pm 2.3 \text{ GeV, NH.} \end{aligned} \tag{8.18}$$

For all QD cases used to obtain mass bounds , we have used the common mass of light neutrinos $m_\nu = 0.23\,\mathrm{eV}$. We find that the bounds obtained from effective mass plots and the half- life plots are in agreement as expected. Also the bounds obtained from the ^{76}Ge data are consistent with those from ^{136}Xe data.

Taking an average of all the bounds and including their uncertainties we find,

$$\overline{\hat{M}}_{S_1} \geq 18.0 \pm 2.9 \text{ GeV.} \tag{8.19}$$

JHEP01(2015)045

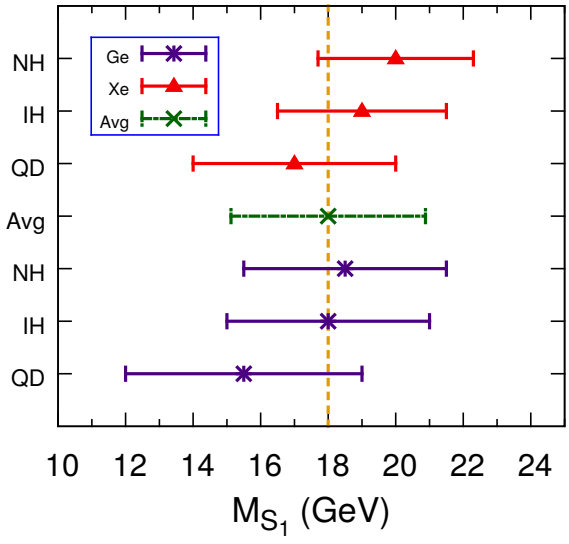

Figure 14. Mass bounds for the lightest sterile neutrino mass $\hat{M}_{S_1}$ obtained from scattered plots of half-life for different light-neutrino mass hierarchies and their comparison with experimental data for ^{76}Ge and ^{136}Xe isotopes cited in the text. The horizontal dashed-green line represents the average value $\overline{\hat{M}}_{S_1} \geq 18.0 \pm 2.9$ GeV. The vertical dashed-red line passing through the average is to guide the eye.

9 TeV scale Z' through flipped SU(5) $\times$ $\tilde{\text{U}}$(1) path

As early as 1980 Witten suggested two-loop generation mechanism in non-SUSY SO(10) for heavy RH Majorana neutrino mass lighter than the GUT scale which is essential in explaining light neutrino masses through type-I seesaw [116]. Quite recently the Witten mechanism has been found to play a significant role in non-SUSY flipped SU(5) model [117] while different aspects of the model have been discussed by a number of authors earlier [118–121]. Several advantages of the model including those relating to proton decay predictions have been discussed in refs. [117, 121]. For example, a good advantage of these models is that the dim.6 proton decay operator in the $p \to e^+\pi^0$ mode receives contribution from only one effective operator of the type $\propto \overline{d^c}Q\overline{u^c}L$ making the lifetime prediction much more predictive. However one clear disadvantage compared to all GUTs is that the two gauge couplings of SU(5) and $\tilde{U}(1)$ do not unify into the SO(10) gauge coupling. In these models the Z' mass is either at the SU(5) gauge boson mass scale [117] or at the intermediate scale $\simeq 10^{11}$ GeV [120] while the type-I seesaw controls the light neutrino masses and mixings. Besides showing how TeV scale Z' accessible to LHC and ILC, and gauged inverse seesaw mechanism can be easily accommodated within flipped SU(5) model descending from non-SUSY SO(10) [118, 119] in the un-unified approach, as a new realisation of this work, we show for the first time how the two gauge couplings of the flipped SU(5) $\times$ $\tilde{\text{U}}$(1)($\equiv G_{51}$) are merged into the SO(10) gauge coupling. In the latter case we find that we have to relax the condition of minimal fine-tuning hypothesis. The SO(10) Higgs representations

JHEP01(2015)045

$45_H, 16_H, 10_H$ and the fermion representation 16 decompose under flipped $\mathrm{SU}(5) \times \tilde{\mathrm{U}}(1)$ as

$$\begin{aligned} 45_H &= (24, 0) + (10, -4) + (10, 4) + (1, 0), \\ 16_H \text{ or } 16 &= (10, 1) + (5^*, -3) + (1, 5), \\ 10_H &= (5, -2) + (\bar{5}, 2), \end{aligned} \tag{9.1}$$

and also $126_H \supset (50_H, -2)$ which plays an important role in achieving extended seesaw mechanism in conjunction with $16_H \supset (10, 1)$. Under $\mathrm{SU}(5) \times \tilde{\mathrm{U}}(1)$, the SM fermions are

$$(\bar{5}_F, -3) = \left\{ u^C, \begin{pmatrix} \nu_e \\ e \end{pmatrix} \right\}, \ (10_F, 1) = \left\{ d^C, \begin{pmatrix} u \\ d \end{pmatrix}, \nu^C \right\}, \ (1_F, 5) = \{ e^C \}. \tag{9.2}$$

The $\mathrm{U}(1)_Q$ charge is defined as

$$Q = T_3 - \frac{1}{5} Y' + \frac{1}{5} \tilde{Y}. \tag{9.3}$$

These hyper-charges are normalized in GUT framework as $Y' \to \sqrt{\frac{3}{5}} Y'$ and $\tilde{Y} \to \frac{1}{2\sqrt{10}} \tilde{Y}$. We consider two spontaneous symmetry breaking schemes.

I. Single step breaking of flipped $\mathrm{SU}(5) \times \tilde{\mathrm{U}}(1)$ to SM

$$\mathrm{SO}(10) \xrightarrow[45_H]{M_{10}} \mathrm{SU}(5) \times \tilde{\mathrm{U}}(1) \xrightarrow[10_H]{M_U} \mathrm{SM} \tag{9.4}$$

II. Two step breaking of flipped $\mathrm{SU}(5) \times \tilde{\mathrm{U}}(1)$ to SM

$$\mathrm{SO}(10) \xrightarrow[45_H]{M_{10}} \mathrm{SU}(5) \times \tilde{\mathrm{U}}(1) \xrightarrow[24_H]{M_5} \mathrm{SU}(3)_C \times \mathrm{SU}(2)_L \times \mathrm{U}(1)' \times \tilde{\mathrm{U}}(1) (= G_{3211}) \xrightarrow[10_H, 50_H]{M_{SS}} \mathrm{SM}. \tag{9.5}$$

In both the chains 45_H containing singlet under $\mathrm{SU}(5) \times \tilde{\mathrm{U}}(1)$ acquires VEV of order M_{10}. The VEV of $(24_H, 0) \subset 45_H$ breaks SU(5) but preserves $\tilde{\mathrm{U}}(1)$ symmetry. Since $(10_H, 1) \supset S_{10}(1, 1, 1, 1)$ under G_{3211} and has non-zero charges under each of the U(1)'s in $\mathrm{U}(1)' \times \tilde{\mathrm{U}}(1)$, a VEV along this non-singlet direction breaks $\mathrm{U}(1)' \times \tilde{\mathrm{U}}(1) \to \mathrm{U}(1)_Y$ leading to the SM. The second massive Z' boson is generated at this scale. The G_{3211} submultiplet $S_{50}(1, 1, -2, -2)$ contained in $(50_H, -2)$ also carries out the same intermediate symmetry breaking process independently of the $(10_H, 1)$. As we are interested in low-mass Z' boson we would like to confine to the G_{3211} spontaneous breaking at $1 - 10\,\mathrm{TeV}$. But the two cases differ considerably in quality and minimality as also in the generation of fermion masses having implications for LFV and LNV processes. Intermediate breaking through $(50_H, -2)$ alone generates heavy RH Majorana masses at the tree level at the intermediate scale, but it can not generate $N - S$ mixing mass term. Since the underlying seesaw mechanism is type-I seesaw, the intermediate breaking scale has to be larger than $10^{11}\,\mathrm{GeV}$ which also gives the order of the high scale Z' that is far beyond the limits of LHC or ILC. With such large M_N, LFV and LNV processes are suppressed. Similarly at the tree level $(10_H, 1)$ can not generate TeV scale RH Majorana mass term at the tree level essential for extended seesaw mechanism. Of course the VEV of $(10_H, 1)$ can generate heavy RH

JHEP01(2015)045

neutrino masses which form a Pseudo Dirac pair. In this case inverse seesaw can explain light neutrino masses and LFV. This symmetry breaking has certain minimality property that it needs only small SO(10) representations like $45_H, 16_H$ and 10_H. As we discuss below, this path can give TeV scale Z' accessible to LHC. However when both the VEVs of $(50_H, -2)$ and $(10_H, 1)$ are combined, we achieve TeV scale Z', LFV and LNV decays closer to experimentally accessible values. The light neutrino mass ansatz is provided by the gauged inverse seesaw formula. To visualize the inverse seesaw structure in the theory we add one $\mathrm{SU}(5) \times \tilde{\mathrm{U}}(1)$ singlet fermion per generation $(S_i, i = 1-3)$. We discuss different cases of SO(10) breaking and their phenomenology through $\mathrm{SU}(5) \times \tilde{\mathrm{U}}(1)$ path.

9.1 Single step breaking of flipped $\mathbf{SU(5) \times \tilde{U}(1)}$

If we assume that $\mathrm{SU}(5) \times \tilde{\mathrm{U}}(1)$ symmetry is broken directly to SM by assigning GUT scale VEVs to the SM singlets of $(24_H, 0)$ and $(10_H, 1)$, then for $\alpha_G^{-1} \sim 45$,

$$M_N \simeq 3 \times 10^{10-11} \times M_d. \tag{9.6}$$

This case has been investigated in detail with minimal fermionic and Higgs representations with type-I seesaw ansatz for neutrino masses [117]. Since the Z' mass is near the GUT scale in this model and our interest is LHC accessible Z', we consider the second option of two-step breaking of flipped $\mathrm{SU}(5) \times \tilde{\mathrm{U}}(1)$ to SM.

9.2 Two-step breaking and unification of $\mathbf{SU(5) \times \tilde{U}(1)}$ couplings

9.2.1 Misaligned couplings in the minimal model

As discussed above we implement the first and second steps of breakings of $\mathrm{SO}(10) \to \mathrm{SU}(5) \times \tilde{\mathrm{U}}(1) \to G_{3211}$ by different components contained in the Higgs representation 45_H of SO(10). We then carry out the third step of intermediate breaking through the representation $(50_H, -2) \subset (126_H)$ of SO(10) where the TeV scale Z' boson and heavy RH Majorana masses are generated. The $N - S$ mixing via the smaller VEV of $(10_H, 1)$ guarantees the desired condition $M_N \gg M \gg M_D, \mu_S$ for extended seesaw mechanism. Finally the SM breaks to $\mathrm{SU}(3)_C \times \mathrm{U}(1)_Q$ by the SM doublet in $5_H \subset \mathrm{SU}(5)$ contained in $10_H \subset \mathrm{SO}(10)$. The gauge couplings of the SM and those in $\mathrm{SU}(3)_C \times \mathrm{SU}(2)_L \times \mathrm{U}(1)' \times \tilde{U}(1)$ are governed by the corresponding RGEs in their respective ranges with beta function coefficients

$$a_{3c} = -7,\ a_{2L} = -19/6,\ a_Y = a'_1 = 41/10, a_{\tilde{1}} = 49/10\,. \tag{9.7}$$

At the seesaw scale $\mu = M_{SS}$, the matching condition for the U(1) gauge couplings are,

$$\alpha_Y^{-1} = \frac{24}{25}\alpha_{1'}^{-1} + \frac{1}{25}\alpha_{\tilde{1}}^{-1}. \tag{9.8}$$

The matching condition in this case permits the two inverse fine structure constants in $\mathrm{U}(1)' \times \tilde{\mathrm{U}}(1)$ at $\mu = M_{SS}$ to have somewhat wider separation that almost persists up to the Planck scale. Although the gauge couplings of $G_{321'}$ unify at $M_5 = 10^{17}$ GeV, the $\tilde{\mathrm{U}}(1)$ remains misaligned as shown in figure 15 in the minimal model.

JHEP01(2015)045

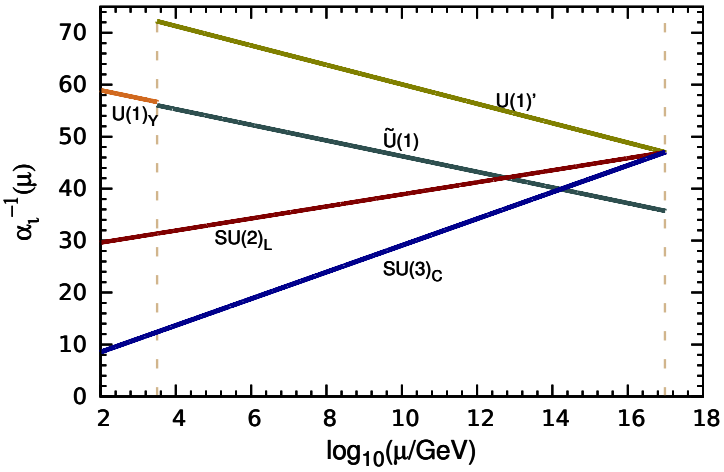

Figure 15. Evolution of gauge couplings in a flipped SU(5) unification theory with a low mass Z' gauge boson mass showing misaligned couplings of SU(5) and $\tilde{U}(1)$.

9.2.2 Unification of SU(5) × Ũ(1) couplings into SO(10)

Although with the minimal content of Higgs scalars, the two gauge couplings of G_{51} remain un-unified, we have obtained successful unification by pulling down the following sets of complex Higgs scalars to their respective lighter mass scales. At the SU(5) unification level besides the Higgs representation $(50_H, 24_H, 10_H, 5_H) \subset \mathrm{SU}(5)$, we include two more complex 24_H representations. From a total number of three 24_H's, we pull out the three Higgs scalar components $\sigma_L(1,3,0,0)$ under G_{3211} to the mass scale $M_\sigma = 500 - 1000\,\mathrm{GeV}$ and two complex scalar components $C_8(8,1,0,0)$ under G_{3211} to the mass scale $10^6\,\mathrm{GeV}$. These are contained in $3(24_H, 0)$ of SU(5) or $3(45_H)$ of SO(10). This procedure of achieving unification in SUSY and non-SUSY models have been adopted in a number of papers earlier [60–64, 122] and also recently [123] in predicting TeV scale RH gauge bosons of left-right gauge theory. In this case although the matching condition eq. (9.8) permits the three U(1) couplings to be nearly equal at $\mu = M_{SS}$, because of the difference in the beta-function coefficients, the two $\mathrm{U}(1)' \times \tilde{U}(1)$ couplings become distinct for $\mu > M_{SS}$ until U(1)′ coupling merges into SU(5) coupling along with g_{2L} and g_{3C} at $M_5 \sim 10^{15.2}\,\mathrm{GeV}$. Finally the two gauge couplings of $\mathrm{SU}(5) \times \tilde{U}(1)$ merge with SO(10) gauge coupling at $\sim 10^{16.5}\,\mathrm{GeV}$. To our knowledge such gauge coupling unification in the SU(5) × Ũ(1) path is first of its kind as presented here.

The evolution of gauge couplings with the VEV $v_\Delta = 10\,\mathrm{TeV}$ is presented in figure 16 which shows that the three gauge couplings in $\mathrm{SU}(3)_C \times \mathrm{SU}(2)_L \times \mathrm{U}(1)'$ unify into SU(5) at $M_5 \sim 10^{15.26}\,\mathrm{GeV}$ whereas the two gauge couplings of SU(5) × Ũ(1) merge with the SO(10) coupling at $M_{10} = 10^{16.56}\,\mathrm{GeV}$.

The beta function coefficients in the presence of these fields and other parameters in

JHEP01(2015)045

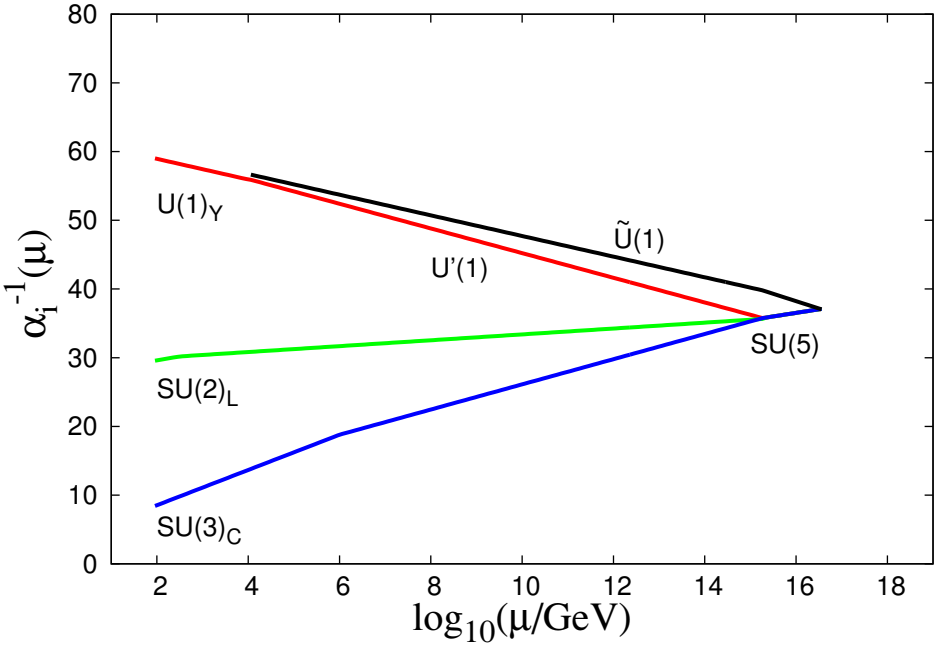

Figure 16. Evolution of gauge couplings in the flipped SU(5) $\times\, \tilde{U}(1)$ path of non-SUSY SO(10) theory showing unification into SU(5) and SO(10) at two different stages with $M_5 \simeq 10^{15.25}\,\mathrm{GeV}$ and $M_{10} = 10^{16.56}\,\mathrm{GeV}$.

this unification scheme are

$$\begin{aligned} a_{2L} &= -7/6, & \mu &> 500\mathrm{GeV}, \\ a_{3C} &= -5, & \mu &> 10^6\mathrm{GeV}, \\ a_5 &= -17/6, & \mu &\geq M_5 = 10^{15.26}\mathrm{GeV} \qquad (9.9) \\ a_{\tilde{\mathrm{U}}(1)} &= 41/10, & 10^4\mathrm{GeV} &\leq \mu \leq 10^{15.256}\mathrm{GeV}, \\ a_{\tilde{\mathrm{U}}(1)} &= 35/6, & M_{10} &\geq \mu \geq M_5 = 10^{15.26}\mathrm{GeV}\,. \qquad (9.10) \end{aligned}$$

The inverse fine-structure constants for SU(5) and SO(10) turn out to be

$$\begin{aligned} \alpha_5^{-1}(M_5) &= 35.8, \\ \alpha_{\tilde{\mathrm{U}}(1)}^{-1}(M_5) &= 39.8, \\ \alpha_{10}^{-1}(M_{10}) &= 37.0. \qquad (9.11) \end{aligned}$$

The values of other coefficients are the same as in minimal case in the corresponding mass ranges. With $X^{\pm 4/3}$ and $Y^{\pm 1/3}$ gauge boson masses at $M_5^0 = 10^{15.26}\,\mathrm{GeV}$, it might be argued at first sight that the proton lifetime prediction for $p \to e^+\pi^0$ with $\tau_P^0 \simeq 5 \times 10^{33}$ yrs is a little less than the current experimental limit. But this deficit is more than compensated by uncertainties from different sources. At first a generic factor contributing to this uncertainty in flipped SU(5) models has been recently noted to be due to the charged lepton mixing matrix. Of course a major source of uncertainty is from threshold effects

JHEP01(2015)045

due to super-heavy scalar components in $(50_H, -2) \subset 126_H$, $3(24_H, 0) \subset 3(45_H)$, $(10_H, 1) \subset 16_H$ and $5_H \subset 10_H$ of SO(10). Including the threshold contributions of SU(5) GUT scale masses of $\S_H = 3[(3, 2, 5/3) + (\bar{3}, 2, -5/3)]$ and ignoring the effects of all other super heavy components for simplicity, we get $M_5 = 10^{15.26\pm0.75}$ which predicts $\tau_{p_{\rm max}} = 4.2 \times 10^{35}$ yrs. for $p \to e^+\pi^0$ mode where we have used M_5/M_{S_H}. In this model the SO(10) superheavy gauge boson are expected to make still larger threshold corrections [49, 50].

10 Lepton flavor and lepton number violations in SU(5) × Ũ(1) path

We write the Yukawa part of the Lagrangian

$$\begin{aligned}
\mathcal{L}_Y &= \mathcal{L}_Y^{(1)} + \mathcal{L}_Y^{(2)}, \\
\mathcal{L}_Y^{(1)} &= Y_{10} 10_F 10_F 5_H + Y_5 10_F \bar{5}_F 5_H^* + Y_1 \bar{5}_F 1_F 5_H + Y_S 10_F 1_S 10_H^* + \mu_S 1_S 1_S + h.c., \\
\mathcal{L}_Y^{(2)} &= Y_{50} 10_F 10_F 50_H + h.c.
\end{aligned} \tag{10.1}$$

This Lagrangian gives $M_D = M_u^T$, $M_d = M_d^T$ and an arbitrary electron mass matrix M_e at the GUT scale. The fourth term in the r.h.s. of the second equation gives $N - S$ mixing term (M) and the RH neutrino matrix $M_N = Y_{50} \langle 50_H \rangle$. Then the full neutrino mass matrix in the (ν, S, N^C) basis can be written as given in eq. (6.1). It is well known that in the limit $M_N \to 0$ the heavy RH neutrino masses in this case form a pseudo-Dirac pair with $M_R = -M \pm \mu_S/2$ and the light neutrino mass matrix is given by the gauged inverse seesaw formula as given in eq. (6.3). In the framework of extended seesaw mechanism, the hierarchy among the elements of eq. (6.1) to achieve inverse seesaw after cancellation of type-I seesaw requires $\mu_S, M_D \ll M \ll M_N$ and $\mathcal{O}(\mu_S M_N) < \mathcal{O}(M^2)$.

10.1 Estimating M_D and $\nu - S$ mixing matrix M

The Yukawa couplings at the GUT scale would not be very different form what we estimate in SM scenario. This is because the only difference appearing in the RGE equations of flipped SU(5) is due to weaker couplings g_1' and $\tilde{g}_1$, and a mild correction due to additional Yukawa terms. In the presence of other free parameters a precise M_D is not necessary.

The Yukawa Lagrangian, as given in eq. (10.1), constrains the fermion masses such that the up-quark and Dirac neutrino mass matrices arising from $10_F \bar{5}_F 5_H^*$ are $M_D = M_u^T$. The down-quark mass matrix arising from a symmetric term $10_f 10_F 5_H$ is $M_d = M_d^T$. The matrix M_d being a complex symmetric matrix is diagonalized by a single unitary matrix L_d with $M_d = L_d \hat{M}_d L_d^T$ where $\hat{M}_d$ is a diagonal matrix. We also note that electron mass matrix M_e and the $N - S$ mixing matrix M arising from $\bar{5}_F 1_F 5_H$ and $10_F 1_S 10_H^*$, respectively, are arbitrary. Similarly μ_S and M_N are complex symmetric matrices arising from $1_S 1_S$ and $10_F 10_F 50_H$, respectively. An arbitrary complex matrix (say A) is diagonalized using bi-unitary transformation $A = L_A \hat{A} R_A^\dagger$. Within the SM we never require information of right unitary matrices and hermitian structures $Y_A Y_A^\dagger$ for $A = u, d, e$ is diagonalized by only one unitary matrix. The CKM matrix is defined as $V_{\rm CKM} = L_u^\dagger L_d$. Throughout the evolution from M_Z scale to GUT scale, these hermitian matrices remain hermitian. In

the theories beyond the standard model we, sometimes, require the information of right diagonalizing matrices too, but, we do not have any mechanism to do that.

Though we can estimate $\hat{M}_d, \hat{M}_u$ and $V_{\rm CKM}$, the matrix M_u is ambiguous. The LFV and LNV depend on M_D matrix, therefore the choice of M_u is crucial. For simplicity we assume $M_u(M_{\rm GUT})$ to be hermitian. We either choose $M_d(M_Z) = \hat{M}_d(M_Z)$ (Case-A) or $M_u(M_Z) = \hat{M}_u(M_Z)$ (Case-B). Also since M_D does not evolve much we assume for all practical purposes that $M_D(M_{SS}) \simeq M_D(M_{\rm GUT})$. The Dirac mass matrix for Case-A is

$$M_D = \begin{pmatrix} 0.0175 & -0.0736 + 0.0098i & 0.5844 - 0.2295i \\ -0.0736 - 0.0098i & 0.3354 & -2.929 - 0.0532i \\ 0.5844 + 0.2295i & -2.929 + 0.0532i & 72.0526 \end{pmatrix} \text{GeV}, \tag{10.2}$$

and for Case-B, it is

$$M_D = \begin{pmatrix} 0.00046668 & (-1.02 - 1.04i) \times 10^{-9} & (-2.93 - 7.56i) \times 10^{-6} \\ (-1.02 + 1.04i) \times 10^{-9} & 0.22746 & -9.567 \times 10^{-5} \\ (-2.93 + 7.56i) \times 10^{-6} & -9.567 \times 10^{-5} & 72.1775 \end{pmatrix} \text{GeV}. \tag{10.3}$$

Irrespective of the scale of M_N, if the condition $\mu_S M_N \ll M^2$ is satisfied and if $\mu_S < M_D \ll M$ is maintained, the neutrino masses and mixings are expressed by the eq. (6.3). For simplicity, we assume diagonal M and M_N matrices at the seesaw scale.

10.2 Lepton flavor violation and neutrinoless double beta decay

The branching ratios can be estimated using eq. (7.1). For $N - S$ mixing matrix $M = \text{diag}(100, 500, 1000)$ GeV and heavy Majorana mass matrix $M_N = \text{diag}(500, 2000, 5000)$ GeV in Case-A we have estimated the branching ratios

$$\begin{aligned} \text{Br}(\mu \to e\gamma) &= 9.6 \times 10^{-16}, \\ \text{Br}(\tau \to e\gamma) &= 1.0 \times 10^{-13}, \\ \text{Br}(\tau \to \mu\gamma) &= 2.2 \times 10^{-12}, \end{aligned} \tag{10.4}$$

while in Case-B they are

$$\begin{aligned} \text{Br}(\mu \to e\gamma) &= 7.8 \times 10^{-33}, \\ \text{Br}(\tau \to e\gamma) &= 1.7 \times 10^{-23}, \\ \text{Br}(\tau \to \mu\gamma) &= 2.4 \times 10^{-21}. \end{aligned} \tag{10.5}$$

The Dirac mass matrix in Case-B is almost diagonal and $(M_D)_{11}$ in this case is almost 40 times smaller than $(M_D)_{11}$ in Case-A. Therefore, LFV branching ratio as well as neutrinoless double beta decay (for the above M matrix) in Case-B will be much smaller compared to Case-A. In the absence M_N and for the same M as above, the two cases give:
Case-A

$$\begin{aligned} \text{Br}(\mu \to e\gamma) &= 2.7 \times 10^{-15}, \\ \text{Br}(\tau \to e\gamma) &= 2.8 \times 10^{-13}, \\ \text{Br}(\tau \to \mu\gamma) &= 6.0 \times 10^{-12}. \end{aligned} \tag{10.6}$$

JHEP01(2015)045

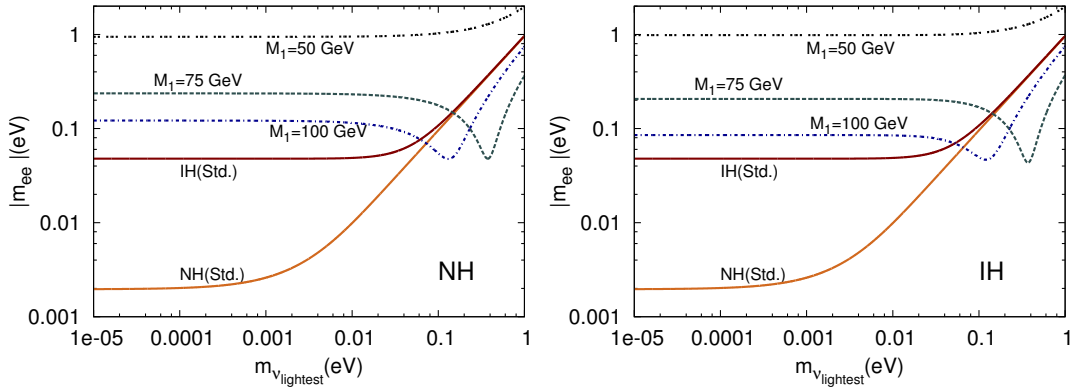

Figure 17. The effective mass parameter vs lightest neutrino mass in the flipped SU(5) path with TeV scale Z' boson with $|p| \simeq 190\,\text{MeV}$. and for $M_N = \text{diag}(500, 2000, 5000)\,\text{GeV}$ and $M = \text{diag}(M_1, 500, 1000)\,\text{GeV}$ while $\mu_S, M_D \ll M < M_N$. In the left panel dashed lines correspond to NH-standard + sterile contribution, and in the right panel they correspond to IH-standard + sterile contribution.

Case-B

$$\begin{aligned} \text{Br}(\mu \to e\gamma) &= 2.4 \times 10^{-34}, \\ \text{Br}(\tau \to e\gamma) &= 4.4 \times 10^{-23}, \\ \text{Br}(\tau \to \mu\gamma) &= 6.3 \times 10^{-21}. \end{aligned} \tag{10.7}$$

which are not very different from the case in which $M_N (\gg M)$ was present.

For the Case-A, the $0\nu\beta\beta$-decay effective masses are shown in figure 17, where solid curves correspond to standard contribution by active neutrinos for the best fit values of oscillation parameters. The dashed curves correspond to the standard + sterile contributions. Dips in the dashed curves are due to cancellation among standard and sterile contributions. The scalar 50_H is necessary to get a new contribution to $0\nu\beta\beta$-decay beyond the standard one. In absence of M_N while heavy neutrinos acquire pseudo-Dirac masses, the new $0\nu\beta\beta$-decay contributions are absent.

The new $0\nu\beta\beta$-decay contributions in Case-B can be made significant for a different choice of M and M_N matrices. For simplicity we still assume them to be diagonal. Using the non-unitarity constraints on the diagonal elements, η_{11}, η_{22} and η_{33}, we find that $M = \text{diag}(0.0075, 5.75, 992)\,\text{GeV}$ is permissible. For this choice of M we estimate $0\nu\beta\beta$-decay effective masses for two choices of M_N: $M_N \ll M$ and $M_N \gg M$.

For various choices of M_N the effective masses are estimated and presented in figure 18. For $M = \text{diag}(0.0075, 5.75, 992)\,\text{GeV}$ and $M_N = \text{diag}(1000, 2000, 2000)\,\text{GeV}$, we get sterile neutrino masses $\hat{M}_S = (55 \times 10^{-9}, 16.56 \times 10^{-3}, 410)\,\text{GeV}$, and heavy RH neutrino masses $\hat{M}_N = (1000, 2000, 2410)\,\text{GeV}$. The details of analysis on $0\nu\beta\beta$-decay can be carried out following section 8.

JHEP01(2015)045

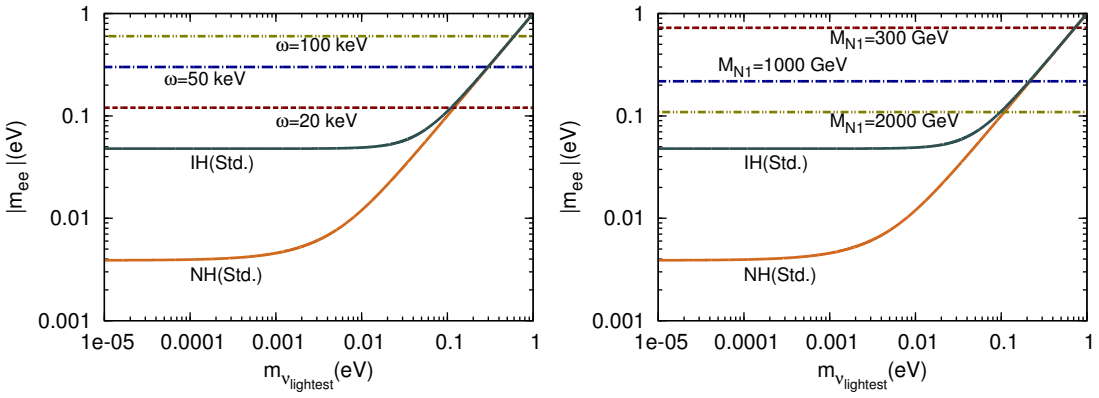

Figure 18. The effective mass as a function of lightest neutrino mass. The matrix $M = \text{diag}(0.0075, 5.75, 992)\,\text{GeV}$. For the left panel we have taken $M_N = \omega 1$ and for the right panel $(M_{N2}, M_{N3}) \gg (M_2, M_3)$. Only M_{N1} affects the effective mass. The exchange momentum $|p| \simeq 190\,\text{MeV}$.

11 Summary and discussions

We have implemented extended seesaw mechanism in a class of SO(10) models containing one additional fermion singlet (S) per generation leading to TeV scale Z' boson and heavy RH Majorana neutrino (N) masses. Our investigations carried out in this work are broadly divided into two categories: (a) SO(10) breaking along the Pati-Salam path and (b) SO(10) breaking along the flipped SU(5) $\times \tilde{U}(1)$ path. Under the category (a) the Z' boson is generated via $\text{U}(1)_R \times \text{U}(1)_{B-L}$ gauge symmetry breaking through the Higgs representation 126_H while the $N - S$ mixing matrix M is generated through the VEV of RH doublet Higgs contained in 16_H. In spite of the presence of the TeV scale RH neutrino mass matrix M_N, and naturally dominant Dirac neutrino mass matrix (M_D) in the model, the would-be large contribution due to type-I seesaw cancels out. The type-II seesaw contribution is damped out because of large parity violating scale and the TeV scale $B - L$ breaking. The formula for light left-handed neutrino masses and mixings are adequately well represented by the gauged inverse seesaw formula . The Dirac neutrino mass matrix M_D that plays a crucial role in the inverse seesaw formula, non-unitarity effects and predictions of LFV decays and $0\nu\beta\beta$ decay is obtained by fitting the charged fermion masses and CKM mixings at the GUT scale for which the induced VEV of $\xi(2, 2, 15) \subset 126_H$ is utilized in addition to two separate Higgs doublets originating from $10_{H_{(1,2)}}$. The roles of two different types of SO(10) structures corresponding to the presence of (i) a single representation 126_H leading to a diagonal structure of RH neutrino mass matrix, or (ii) two representations 126_H and $126'_H$ leading to a general structure of RH neutrino mass matrix, are discussed with their respective impact on the phenomenology of observable $n - \bar{n}$ oscillation. While the dominant new contribution to $0\nu 2\beta$ decay in the $W_L - W_L$ channel due to sterile neutrino exchanges, saturates the current experimental limits arrived at various experimental groups, the branching ratios for LFV decays, and rare kaon decays are noted to be within the accessible ranges of ongoing search experiments. Using RG

JHEP01(2015)045

analysis, we have derived the lower bound on the lepto-quark gage boson mass mediating rare kaon decays to be $M_{\rm LQ} \geq (1.54 \pm 0.06) \times 10^6\,{\rm GeV}$ which is easily accommodated in the GUT scenario. The unification constraint on gauge couplings of the SO(10) model is found to permit diquark Higgs scalar masses extending from $\sim$ (10-100) TeV leading to observable $n - \bar{n}$ oscillation while satisfying flavor physics constraints [115] saturating the lepto-quark gauge boson mass bound. These suggest that the model is also simultaneously consistent with observable rare kaon decay by ongoing search experiments.

Compared to the recent interesting proposal of refs. [29–31], although successful generation of baryon asymmetry of the universe has not been implemented so far in this model, we have one extra gauge boson accessible to LHC. Likewise, in our model the lepto-quark gauge boson mediated $K_L \to \mu\bar{e}$ is also accessible to ongoing search experiments. Whereas the new $B - L$ violating proton decay is predicted to be accessible in refs. [29–31], in our case it is $B - L$ conserving proton decay $p \to e^+\pi^0$. Whereas the type-I seesaw mechanism associated with high $B - L$ breaking scale is generally inaccessible to direct experimental tests, in our case the TeV-scale gauged inverse seesaw is directly verifiable. In the minimal model the predicted values of the RH neutrino masses are also accessible for verification at LHC.

Even though the model is non-supersymmetric, it predicts similar branching ratios as in SUSY models for LFV processes like $\mu \to e\gamma$, $\tau \to \mu\gamma$, and $\tau \to e\gamma$. Even for the Dirac phase $\delta = 0, \pi, 2\pi$ of the PMNS matrix, the model predicts the leptonic CP-violation parameter $J \simeq 10^{-5}$ due to non-unitarity effects. We have explicitly derived a new formula for the half life of $0\nu\beta\beta$ decay as a function of the sterile neutrino masses in the model and derived the lower bound $\hat{M}_{S_1} \geq 18 \pm 2.9\,{\rm GeV}$ imposed by the current experimental limits on the half life. In this model the lifetime corresponding to Heidelberg Moscow experiment does not necessarily require the light neutrinos to be quasi-degenerate.

The predicted proton-lifetime in the minimal model is found to be $\tau_p(p \to e^+\pi^0) \simeq 5.05 \times 10^{35\pm1.0\pm0.34}$yrs where the first (second) uncertainty is due to GUT-threshold effects (experimental errors). This lifetime is accessible to ongoing and planned experiments. We have noted significant reduction of the predicted lifetime, bringing the central value much closer to the current Super K. limit with $\tau_p(p \to e^+\pi^0) = 1.1 \times 10^{34}{\rm yrs} - 5.05 \times 10^{35}$ yrs when the effect of a lighter bi-triplet Higgs contained in the representation $54_H \subset {\rm SO}(10)$ is included. We conclude that even though the model does not have low-mass RH $W_R^\pm$ bosons in the accessible range of LHC, it is associated with interesting signatures on lepton flavor, lepton number and baryon number violations, and rare kaon decays along with the LHC accessible Z' boson.

Under the category (b) the TeV -scale Z' boson is generated via spontaneous symmetry breaking of the subgroup ${\rm U}(1)' \times \tilde{U}(1) \to {\rm U}(1)_Y$. For the first time we have successfully unified the two gauge couplings of ${\rm SU}(5) \times \tilde{U}(1)$ into the SO(10) gauge coupling at $M_{10} = 10^{16.6}\,{\rm GeV}$. The three gauge couplings of ${\rm SU}(3)_C \times {\rm SU}(2)_L \times {\rm U}(1)'$ in this case unify into the SU(5) gauge coupling at $M_5 = 10^{15.26}\,{\rm GeV}$. Including small threshold effects the predicted proton lifetime is easily accessible to ongoing searches in this model. Although this model does not predict observable $n - \bar{n}$ oscillation or rare kaon decays, it predicts a rich structure of experimentally observable lepton number as well as charged lepton flavor violations. As

JHEP01(2015)045

in the case of the symmetry breaking through the Pati-Salam route, saturation of the expetrimental data on effective mass parameter or half-life for $0\nu\beta\beta$ decay in this case also does not require the light neutrinos to be quasi-degenerate.

A Formulas for threshold effects

A.1 Estimation of experimental and GUT-threshold uncertainties on the unification scale

A.1.1 Analytic formulas

In contrast to other intermediate gauge symmetries, SO(10) model with G_{224D} intermediate symmetry was noted to have the remarkable property that GUT threshold corrections arising out of superheavy masses or higher dimensional operators identically vanish on $\sin^2\theta_W$ or the G_{224D} breaking scale [53, 54, 57, 59]. We show how this property can be ensured in this model with precision gauge coupling unification while predicting vanishing GUT-threshold corrections on M_P, analytically, but with non-vanishing finite corrections on M_{GUT}. We derive the corresponding GUT threshold effects in SO(10) model with three intermediate symmetry breaking steps, G_{224D}, G_{224}, and G_{2113} between the GUT and the standard model whereas the uncertainties in the mass scales has been discussed in ref. [58] only with single intermediate breaking. The symmetry breaking chain under consideration is

$$\mathrm{SO}(10) \xrightarrow[M_U]{a_i'''} G_{224D} \xrightarrow[M_P]{a_i''} G_{224} \xrightarrow[M_C]{a_i'} G_{2113} \xrightarrow[M_R^0]{a_i} G_{\mathrm{SM}} \xrightarrow[M_Z]{} G_{13}, \tag{A.1}$$

where a_i''', a_i'', a_i', and a_i are, respectively, the one-loop beta coefficients for the gauge group $G_{2_L2_R4_CD}$, $G_{2_L2_R4_C}$, $G_{2_L1_R1_{B-L}3_C}$, and $G_{\mathrm{SM}} \equiv G_{2_L1_Y3_C}$.

Following the formalism used in refs. [58, 59], one can write the expressions for two different contributions of $\sin^2\theta_W\,(M_Z)$, and $\alpha_s\,(M_Z)$:

$$16\pi\left(\alpha_s^{-1} - \frac{3}{8}\alpha_{\mathrm{em}}^{-1}\right) = \mathcal{A}_P \ln\left(\frac{M_P}{M_Z}\right) + \mathcal{A}_U \ln\left(\frac{M_U}{M_Z}\right) + \mathcal{A}_C \ln\left(\frac{M_C}{M_Z}\right) + \mathcal{A}_0 \ln\left(\frac{M_R^0}{M_Z}\right) + f_M^U, \tag{A.2}$$

where,

$$\begin{aligned}
\mathcal{A}_0 &= (8a_{3C} - 3a_{2L} - 5a_Y) - \left(8a'_{3C} - 3a'_{2L} - 3a'_{1R} - 2a'_{B-L}\right)\,, \\
\mathcal{A}_C &= \left(8a'_{3C} - 3a'_{2L} - 3a'_{1R} - 2a'_{B-L}\right) - \left(6a''_{4C} - 3a''_{2L} - 3a''_{2R}\right)\,, \\
\mathcal{A}_P &= \left(6a''_{4C} - 3a''_{2L} - 3a''_{2R}\right) - \left(6a'''_{4C} - 6a'''_{2L}\right)\,, \\
\mathcal{A}_U &= \left(6a'''_{4C} - 6a'''_{2L}\right)\,, \\
f_M^U &= \lambda_{2L}^U - \lambda_{4C}^U\,.
\end{aligned}$$

Similarly,

$$16\pi\,\alpha_{\mathrm{em}}^{-1}\left(\sin^2\theta_W - \frac{3}{8}\right) = \mathcal{B}_P \ln\left(\frac{M_P}{M_Z}\right) + \mathcal{B}_U \ln\left(\frac{M_U}{M_Z}\right) + \mathcal{B}_C \ln\left(\frac{M_C}{M_Z}\right) + \mathcal{B}_0 \ln\left(\frac{M_R^0}{M_Z}\right) + f_\theta^U\,, \tag{A.3}$$

JHEP01(2015)045

with

$$\begin{aligned}
\mathcal{B}_0 &= (5a_{2L} - 5a_Y) - \left(5a'_{2L} - 3a'_{1R} - 2a'_{B-L}\right) , \\
\mathcal{B}_C &= \left(5a'_{2L} - 3a'_{1R} - 2a'_{B-L}\right) - \left(5a''_{2L} - 3a''_{2R} - 2a''_{4C}\right) , \\
\mathcal{B}_P &= \left(5a''_{2L} - 3a''_{2R} - 2a''_{4C}\right) - \left(2a'''_{2L} - 2a'''_{4C}\right) , \\
\mathcal{B}_U &= \left(2a'''_{2L} - 2a'''_{4C}\right) , \\
f^U_\theta &= \frac{1}{3}\left(\lambda^U_{4C} - \lambda^U_{2L}\right) .
\end{aligned}$$

It is well known that threshold effects at intermediate scales are likely to introduce discontinuities in the gauge couplings thereby destroying possibilities of precision unification. This fact has led us to restrict the model with vanishing intermediate scale threshold corrections by assuming relevant sub-multiplets to have masses exactly equal to their respective intermediate scales which is applicable to the intermediate scales M^0_R, M^+_R, and M_C in the present work.

Denoting $\mathcal{C}_0 = 16\pi\left(\alpha_s^{-1} - \frac{3}{8}\alpha_{\rm em}^{-1}\right)$, and $\mathcal{C}_1 = 16\pi\,\alpha_{\rm em}^{-1}\left(\sin^2\theta_W - \frac{3}{8}\right)$, one can rewrite the eq. (A.2), and eq. (A.3) for M_P and M_U as

$$\mathcal{A}_P \ln\left(\frac{M_P}{M_Z}\right) + \mathcal{A}_U \ln\left(\frac{M_U}{M_Z}\right) = \mathcal{D}_0 = \mathcal{C}_0 - \mathcal{A}_C \ln\left(\frac{M_C}{M_Z}\right) - \mathcal{A}_0 \ln\left(\frac{M^0_R}{M_Z}\right) - f^U_M \,, \tag{A.4}$$

$$\mathcal{B}_P \ln\left(\frac{M_P}{M_Z}\right) + \mathcal{B}_U \ln\left(\frac{M_U}{M_Z}\right) = \mathcal{D}_1 = \mathcal{C}_1 - \mathcal{B}_C \ln\left(\frac{M_C}{M_Z}\right) - \mathcal{B}_0 \ln\left(\frac{M^0_R}{M_Z}\right) - f^U_\theta \,. \tag{A.5}$$

A formal solution for these two sets of eqs. (A.4), and (A.5),

$$\ln\left(\frac{M_U}{M_Z}\right) = \frac{\mathcal{D}_1\mathcal{A}_P - \mathcal{D}_0\mathcal{B}_P}{\mathcal{B}_U\mathcal{A}_P - \mathcal{A}_U\mathcal{B}_P} \,, \tag{A.6}$$

$$\ln\left(\frac{M_P}{M_Z}\right) = \frac{\mathcal{D}_0\mathcal{B}_U - \mathcal{D}_1\mathcal{A}_U}{\mathcal{B}_U\mathcal{A}_P - \mathcal{A}_U\mathcal{B}_P} \,. \tag{A.7}$$

In this present work, we derive two types of uncertainties in the mass scales of SO(10) model; i.e, the first one comes from low energy parameters taken from their experimental errors and another one arising from the threshold corrections accounting the theoretical uncertainties in the mass scales due to heavy Higgs fields present at GUT scale. These two categories are presented below:

A.1.2 Uncertainties due to experimental errors in $\sin^2\theta_W$ and α_s

In eqs. (A.4) and (A.5) the low energy parameters are contained in $\mathcal{C}_0$ and $\mathcal{C}_1$. As a result, we have got further simplified relations relevant for experimental uncertainties, i.e,

JHEP01(2015)045

$\Delta(\mathcal{D}_0) = \Delta(\mathcal{C}_0)$ and $\Delta(\mathcal{D}_1) = \Delta(\mathcal{C}_1)$, and hence,

$$\Delta \ln\left(\frac{M_U}{M_Z}\right)\Big|_{\text{expt.}} = \frac{\Delta(\mathcal{C}_1)\,\mathcal{A}_P - \Delta(\mathcal{C}_0)\,\mathcal{B}_P}{\mathcal{B}_U\mathcal{A}_P - \mathcal{A}_U\mathcal{B}_P}$$
$$= \frac{\left[(16\pi)\,\alpha_{\text{em}}^{-1}(\delta \sin^2\theta_W)\right]\mathcal{A}_P - \left[-\frac{(16\pi)}{\alpha_s^2}\,(\delta\alpha_s)\right]\mathcal{B}_P}{\mathcal{B}_U\mathcal{A}_P - \mathcal{A}_U\mathcal{B}_P}\,, \tag{A.8}$$

$$\Delta \ln\left(\frac{M_P}{M_Z}\right)\Big|_{\text{expt.}} = \frac{\Delta(\mathcal{C}_0)\,\mathcal{B}_U - \Delta(\mathcal{C}_1)\,\mathcal{A}_U}{\mathcal{B}_U\mathcal{A}_P - \mathcal{A}_U\mathcal{B}_P}$$
$$= \frac{\left[-\frac{(16\pi)}{\alpha_s^2}\,(\delta\alpha_s)\right]\mathcal{B}_U - \left[(16\pi)\,\alpha_{\text{em}}^{-1}(\delta \sin^2\theta_W)\right]\mathcal{A}_U}{\mathcal{B}_U\mathcal{A}_P - \mathcal{A}_U\mathcal{B}_P}\,, \tag{A.9}$$

where, the errors in the experimental values on electroweak mixing angle $\sin^2\theta_W$ and strong coupling constant α_s as $\sin^2\theta_W = 0.23102 \mp 0.00005$, $\alpha_s = 0.118 \pm 0.003$ giving $\delta\alpha_s = \pm 0.003$ and $\delta \sin^2\theta_W = \mp 0.00005$.

A.1.3 Uncertainties in M_U with vanishing correction on M_P

In the present work, we have considered minimal set of Higgs fields belonging to a larger SO(10) Higgs representation implying other Higgs fields which do not take part in symmetry breaking will automatically present at GUT scale. Since we can not determine the masses of these heavy Higgs bosons and, hence, they introduce uncertainty in other mass scales M_P and M_U via renormalization group equations leading to GUT threshold uncertainty in our predictions for proton life time. For this particular model, the GUT threshold corrections to D-parity breaking scale and unification mass scale is presented below

$$\Delta\ln\left(\frac{M_U}{M_Z}\right)\Big|_{\text{GUT Th.}} = \frac{\Delta(\mathcal{D}_1)\,\mathcal{A}_P - \Delta(\mathcal{D}_0)\,\mathcal{B}_P}{\mathcal{B}_U\mathcal{A}_P - \mathcal{A}_U\mathcal{B}_P}$$
$$= \frac{-f_M^U}{6\left(a_{2L}''' - a_{4C}'''\right)}\,, \tag{A.10}$$

$$\Delta\ln\left(\frac{M_P}{M_Z}\right)\Big|_{\text{GUT Th.}} = \frac{\Delta(\mathcal{D}_0)\,\mathcal{B}_U - \Delta(\mathcal{D}_1)\,\mathcal{A}_U}{\mathcal{B}_U\mathcal{A}_P - \mathcal{A}_U\mathcal{B}_P}$$
$$= \frac{\mathcal{B}_U\, f_M^U - \mathcal{A}_U\, f_\theta^U}{24\,\left(a_{2L}''' - a_{4C}'''\right)\left(a_{2L}'' - a_{4C}''\right)} = 0\,. \tag{A.11}$$

The last step resulting in vanishing GUT-threshold correction analytically follows by using expressions for f_M^U, f_θ^U, $\mathcal{B}_U$ and $\mathcal{A}_U$ derived in sub-sub section A.1.1. This was proved in ref. [57].

Acknowledgments

Ram Lal Awasthi acknowledges hospitality at the Center of Excellence in Theoretical and Mathematical Sciences, SOA University where this work was initiated and completed. M.K.P. acknowledges the grant of research project No.SB/S2/HEP-011/2013 by the Government of India.

JHEP01(2015)045

Group G_I	Higgs content	a_i	b_{ij}
$G_{1_Y 2_L 3_C}$	$\Phi(\frac{1}{2}, 2, 1)_{10}$	$\begin{pmatrix} 41/10 \\ -19/6 \\ -7 \end{pmatrix}$	$\begin{pmatrix} 199/50 & 27/10 & 44/5 \\ 9/10 & 35/6 & 12 \\ 11/10 & 9/2 & -26 \end{pmatrix}$
$G_{1_{B-L} 1_R 2_L 3_C}$	$\Phi_1(0, \frac{1}{2}, 2, 1)_{10} \oplus \Phi_2(0, -\frac{1}{2}, 2, 1)_{10'}$ $\Delta_R(-1, 1, 1, 1)_{126} \oplus \chi_R(-\frac{1}{2}, \frac{1}{2}, 1, 1)_{16}$	$\begin{pmatrix} 37/8 \\ 57/12 \\ -3 \\ -7 \end{pmatrix}$	$\begin{pmatrix} 209/16 & 63/8 & 9/4 & 4 \\ 63/8 & 33/4 & 3 & 12 \\ 3/2 & 1 & 8 & 12 \\ 1/2 & 3/2 & 9/2 & -26 \end{pmatrix}$
$G_{2_L 2_R 4_C}$	$\Phi_1(2, 2, 1)_{10} \oplus \Phi_2(2, 2, 1)_{10'}$ $\Delta_R(1, 3, \overline{10})_{126} \oplus \chi_R(1, 2, \overline{4})_{16}$ $\sigma_R(1, 3, 15)_{210}$	$\begin{pmatrix} -8/3 \\ 29/3 \\ -16/3 \end{pmatrix}$	$\begin{pmatrix} 37/3 & 6 & 45/2 \\ 6 & 1103/3 & 1275/2 \\ 9/2 & 255/2 & 736/3 \end{pmatrix}$
$G_{2_L 2_R 4_C D}$	$\Phi_1(2, 2, 1)_{10} \oplus \Phi_2(2, 2, 1)_{10'}$ $\Delta_L(3, 1, 10)_{126} \oplus \Delta_R(1, 3, \overline{10})_{126}$ $\chi_L(2, 1, 4)_{16} \oplus \chi_R(1, 2, \overline{4})_{16}$ $\sigma_L(3, 1, 15)_{210} \oplus \sigma_R(1, 3, 15)_{210}$ $\xi(2, 2, 15)_{126/126'}$	$\begin{pmatrix} 44/3 \\ 44/3 \\ 16/3 \end{pmatrix}$	$\begin{pmatrix} 1298/3 & 51 & 1755/2 \\ 51 & 1298/3 & 1755/2 \\ 351/2 & 351/2 & 1403/2 \end{pmatrix}$

Table 6. One and two loop beta coefficients for different gauge coupling evolutions described in text taking the second Higgs doublet at $\mu \geq 5\,\text{TeV}$.

References

[1] P.A.M. Dirac, *The Fundamental Equations for Quantum Mechanics*, *Proc. Roy. Soc. Lond.* **109** (1925) 752, pg. 642–653.

[2] E. Majorana, *Theory of the Symmetry of Electrons and Positrons*, *Nuovo Cim.* **14** (1937) 171 [INSPIRE].

[3] H.V. Klapdor-Kleingrothaus, *Seventy years of double beta decay:From nuclear physics to beyond-standard-model particle physics*, World Scientific Pub., Hackensack, U.S.A. (2010).

[4] H.V. Klapdor-Kleingrothaus et al., *Latest results from the Heidelberg-Moscow double beta decay experiment*, *Eur. Phys. J.* **A 12** (2001) 147 [hep-ph/0103062] [INSPIRE].

[5] IGEX collaboration, C.E. Aalseth et al., *The IGEX Ge-76 neutrinoless double beta decay experiment: Prospects for next generation experiments*, *Phys. Rev.* **D 65** (2002) 092007 [hep-ex/0202026] [INSPIRE].

JHEP01(2015)045

[6] H.V. Klapdor-Kleingrothaus, I.V. Krivosheina, A. Dietz and O. Chkvorets, *Search for neutrinoless double beta decay with enriched Ge-76 in Gran Sasso 1990–2003*, *Phys. Lett.* **B 586** (2004) 198 [hep-ph/0404088] [INSPIRE].

[7] H.V. Klapdor-Kleingrothaus, I.V. Krivosheina and I.V. Titkova, *Theoretical investigation of pulse shapes of double beta events in a Ge-76 detector, their dependence on particle physics parameters and their separability from background gamma events*, *Mod. Phys. Lett.* **A 21** (2006) 1257 [INSPIRE].

[8] KamLAND-Zen collaboration, A. Gando et al., *Limit on Neutrinoless $\beta\beta$ Decay of Xe-136 from the First Phase of KamLAND-Zen and Comparison with the Positive Claim in Ge-76*, *Phys. Rev. Lett.* **110** (2013) 062502 [arXiv:1211.3863] [INSPIRE].

[9] EXO collaboration, M. Auger et al., *Search for Neutrinoless Double-Beta Decay in ^{136}Xe with EXO-200*, *Phys. Rev. Lett.* **109** (2012) 032505 [arXiv:1205.5608] [INSPIRE].

[10] GERDA collaboration, M. Agostini et al., *Results on Neutrinoless Double-β Decay of ^{76}Ge from Phase I of the GERDA Experiment*, *Phys. Rev. Lett.* **111** (2013) 122503 [arXiv:1307.4720] [INSPIRE].

[11] CUORICINO collaboration, C. Arnaboldi et al., *Results from a search for the 0 neutrino beta beta-decay of Te-130*, *Phys. Rev.* **C 78** (2008) 035502 [arXiv:0802.3439] [INSPIRE].

[12] KATRIN collaboration, A. Osipowicz et al., *KATRIN: A next generation tritium beta decay experiment with sub-eV sensitivity for the electron neutrino mass. Letter of intent*, hep-ex/0109033 [INSPIRE].

[13] Planck collaboration, P.A.R. Ade et al., *Planck 2013 results. XVI. Cosmological parameters*, *Astron. Astrophys.* **571** (2014) A16 [arXiv:1303.5076] [INSPIRE].

[14] P. Minkowski, *$\mu \to e\gamma$ at a Rate of One Out of 1-Billion Muon Decays?*, *Phys. Lett.* **B 67** (1977) 421 [INSPIRE].

[15] T. Yanagida, *Horizontal gauge symmetry and masses of neutrinos*, In Proceedings of the *Workshop on the Baryon Number of the Universe and Unified Theories*, Tsukuba, Japan, 13–14 February 1979.

[16] R.N. Mohapatra and G. Senjanović, *Neutrino Mass and Spontaneous Parity Violation*, *Phys. Rev. Lett.* **44** (1980) 912 [INSPIRE].

[17] J. Schechter and J.W.F. Valle, *Neutrino Masses in* SU(2) × U(1) *Theories*, *Phys. Rev.* **D 22** (1980) 2227 [INSPIRE].

[18] M. Magg and C. Wetterich, *Neutrino Mass Problem and Gauge Hierarchy*, *Phys. Lett.* **B 94** (1980) 61 [INSPIRE].

[19] G. Lazarides, Q. Shafi and C. Wetterich, *Proton Lifetime and Fermion Masses in an* SO(10) *Model*, *Nucl. Phys.* **B 181** (1981) 287 [INSPIRE].

[20] A. Ibarra, E. Molinaro and S.T. Petcov, *TeV Scale See-Saw Mechanisms of Neutrino Mass Generation, the Majorana Nature of the Heavy Singlet Neutrinos and $(\beta\beta)_{0\nu}$-Decay*, *JHEP* **09** (2010) 108 [arXiv:1007.2378] [INSPIRE].

[21] R.N. Mohapatra and J.C. Pati, *A Natural Left-Right Symmetry*, *Phys. Rev.* **D 11** (1975) 2558 [INSPIRE].

[22] J.C. Pati and A. Salam, *Lepton Number as the Fourth Color*, *Phys. Rev.* **D 10** (1974) 275 [*Erratum ibid.* **D 11** (1975) 703-703] [INSPIRE].

JHEP01(2015)045

[23] G. Senjanović and R.N. Mohapatra, *Exact Left-Right Symmetry and Spontaneous Violation of Parity*, *Phys. Rev.* **D 12** (1975) 1502 [INSPIRE].

[24] R.N. Mohapatra and G. Senjanović, *Neutrino Masses and Mixings in Gauge Models with Spontaneous Parity Violation*, *Phys. Rev.* **D 23** (1981) 165 [INSPIRE].

[25] R.N. Mohapatra and R.E. Marshak, *Local B-L Symmetry of Electroweak Interactions, Majorana Neutrinos and Neutron Oscillations*, *Phys. Rev. Lett.* **44** (1980) 1316 [*Erratum ibid.* **44** (1980) 1643] [INSPIRE].

[26] R.N. Mohapatra and G. Senjanović, *Higgs Boson Effects in Grand Unified Theories*, *Phys. Rev.* **D 27** (1983) 1601 [INSPIRE].

[27] R.N. Mohapatra, *Neutron-Anti-Neutron Oscillation: Theory and Phenomenology*, *J. Phys.* **G 36** (2009) 104006 [arXiv:0902.0834] [INSPIRE].

[28] F. del Aguila and L.E. Ibáñez, *Higgs Bosons in* SO(10) *and Partial Unification*, *Nucl. Phys.* **B 177** (1981) 60 [INSPIRE].

[29] K.S. Babu and R.N. Mohapatra, *Coupling Unification, GUT-Scale Baryogenesis and Neutron-Antineutron Oscillation in* SO(10), *Phys. Lett.* **B 715** (2012) 328 [arXiv:1206.5701] [INSPIRE].

[30] K.S. Babu and R.N. Mohapatra, *B-L Violating Nucleon Decay and GUT Scale Baryogenesis in* SO(10), *Phys. Rev.* **D 86** (2012) 035018 [arXiv:1203.5544] [INSPIRE].

[31] K.S. Babu and R.N. Mohapatra, *B-L Violating Proton Decay Modes and New Baryogenesis Scenario in* SO(10), *Phys. Rev. Lett.* **109** (2012) 091803 [arXiv:1207.5771] [INSPIRE].

[32] ATLAS collaboration, *Search for heavy neutrinos and right-handed W bosons in events with two leptons and jets in pp collisions at* $\sqrt{s} = 7$ *TeV with the ATLAS detector*, *Eur. Phys. J.* **C 72** (2012) 2056 [arXiv:1203.5420] [INSPIRE].

[33] CMS collaboration, *Search for heavy neutrinos and* W_R *bosons with right-handed couplings in a left-right symmetric model in pp collisions at* $\sqrt{s} = 7$ *TeV*, *Phys. Rev. Lett.* **109** (2012) 261802 [arXiv:1210.2402] [INSPIRE].

[34] D. Chang, R.N. Mohapatra and M.K. Parida, *Decoupling Parity and* $\mathrm{SU}(2)_R$ *Breaking Scales: A New Approach to Left-Right Symmetric Models*, *Phys. Rev. Lett.* **52** (1984) 1072 [INSPIRE].

[35] D. Chang, R.N. Mohapatra, J. Gipson, R.E. Marshak and M.K. Parida, *Experimental Tests of New* SO(10) *Grand Unification*, *Phys. Rev.* **D 31** (1985) 1718 [INSPIRE].

[36] M.K. Parida, *Natural mass scales for observable matter-antimatter oscillations in* SO(10), *Phys. Lett.* **B 126** (1983) 220 [INSPIRE].

[37] M.K. Parida, *Matter-antimatter oscillations in grand unified theories with high unification masses*, *Phys. Rev.* **D 27** (1983) 2783 [INSPIRE].

[38] BNL collaboration, D. Ambrose et al., *New limit on muon and electron lepton number violation from* $K_L \to \mu^{\pm} e^{\mp}$ *decay*, *Phys. Rev. Lett.* **81** (1998) 5734 [hep-ex/9811038] [INSPIRE].

[39] R.L. Awasthi, M.K. Parida and S. Patra, *Neutrino masses, dominant neutrinoless double beta decay and observable lepton flavor violation in left-right models and* SO(10) *grand unification with low mass* W_R, Z_R *bosons*, *JHEP* **08** (2013) 122 [arXiv:1302.0672] [INSPIRE].

JHEP01(2015)045

[40] C. Arbeláez Rodríguez, H. Kolešová and M. Malinský, *Witten's mechanism in the flipped* SU(5) *unification*, *Phys. Rev.* **D 89** (2014) 055003 [arXiv:1309.6743] [INSPIRE].

[41] C.R. Das, C.D. Froggatt, L.V. Laperashvili and H.B. Nielsen, *Flipped* SU(5)*, see-saw scale physics and degenerate vacua*, *Mod. Phys. Lett.* **A 21** (2006) 1151 [hep-ph/0507182] [INSPIRE].

[42] P. Langacker, *The Physics of Heavy Z' Gauge Bosons*, *Rev. Mod. Phys.* **81** (2009) 1199 [arXiv:0801.1345] [INSPIRE].

[43] T. Han, P. Langacker, Z. Liu and L.-T. Wang, *Diagnosis of a New Neutral Gauge Boson at the LHC and ILC for Snowmass 2013*, arXiv:1308.2738 [INSPIRE].

[44] M.K. Parida and A. Raychaudhuri, *Low Mass Parity Restoration, Weak Interaction Phenomenology and Grand Unification*, *Phys. Rev.* **D 26** (1982) 2364 [INSPIRE].

[45] M.K. Parida and C.C. Hazra, *Left-right Symmetry, $K_L K_S$ Mass Difference and a Possible New Formula for Neutrino Mass*, *Phys. Lett.* **B 121** (1983) 355 [INSPIRE].

[46] O.J.P. Eboli, J. Gonzalez-Fraile and M.C. Gonzalez-Garcia, *Present Bounds on New Neutral Vector Resonances from Electroweak Gauge Boson Pair Production at the LHC*, *Phys. Rev.* **D 85** (2012) 055019 [arXiv:1112.0316] [INSPIRE].

[47] A. Falkowski, C. Grojean, A. Kaminska, S. Pokorski and A. Weiler, *If no Higgs then what?*, *JHEP* **11** (2011) 028 [arXiv:1108.1183] [INSPIRE].

[48] S. Weinberg, *Effective Gauge Theories*, *Phys. Lett.* **B 91** (1980) 51 [INSPIRE].

[49] L.J. Hall, *Grand Unification of Effective Gauge Theories*, *Nucl. Phys.* **B 178** (1981) 75 [INSPIRE].

[50] M.K. Parida, *Heavy Particle Effects in Grand Unified Theories With Fine Structure Constant Matching*, *Phys. Lett.* **B 196** (1987) 163 [INSPIRE].

[51] B.A. Ovrut and H.J. Schnitzer, *Low-energy and threshold calculations using effective field theory*, *Nucl. Phys.* **B 184** (1981) 109 [INSPIRE].

[52] V.V. Dixit and M. Sher, *The Futility of High Precision* SO(10) *Calculations*, *Phys. Rev.* **D 40** (1989) 3765 [INSPIRE].

[53] M.K. Parida and P.K. Patra, *Useful theorem on vanishing threshold contribution to $sin^2_{\theta_W}$ in a class of grand unified theories*, *Phys. Rev. Lett.* **66** (1991) 858 [INSPIRE].

[54] M.K. Parida and P.K. Patra, *Theorem on vanishing multiloop radiative corrections to* $\sin^2_{\theta_W}$ *in grand unified theories at high mass scales*, *Phys. Rev. Lett.* **68** (1992) 754 [INSPIRE].

[55] R.N. Mohapatra, *A theorem on the threshold corrections in grand unified theories*, *Phys. Lett.* **B 285** (1992) 235 [INSPIRE].

[56] P. Langacker and N. Polonsky, *Uncertainties in coupling constant unification*, *Phys. Rev.* **D 47** (1993) 4028 [hep-ph/9210235] [INSPIRE].

[57] M.K. Parida, *Vanishing corrections on intermediate scale and implications for unification of forces*, *Phys. Rev.* **D 57** (1998) 2736 [hep-ph/9710246] [INSPIRE].

[58] R.N. Mohapatra and M.K. Parida, *Threshold effects on the mass scale predictions in* SO(10) *models and solar neutrino puzzle*, *Phys. Rev.* **D 47** (1993) 264 [hep-ph/9204234] [INSPIRE].

JHEP01(2015)045

[59] D.-G. Lee, R.N. Mohapatra, M.K. Parida and M. Rani, *Predictions for proton lifetime in minimal nonsupersymmetric* SO(10) *models: An update*, *Phys. Rev.* **D 51** (1995) 229 [hep-ph/9404238] [INSPIRE].

[60] M.K. Parida and C.C. Hazra, *Superheavy Higgs Scalar Effects in Effective Gauge Theories From* SO(10) *Grand Unification With Low Mass Right-handed Gauge Bosons*, *Phys. Rev.* **D 40** (1989) 3074 [INSPIRE].

[61] M. Rani and M.K. Parida, *Confronting LEP data, proton lifetime and small neutrino masses by threshold effects in* SO(10) *with* $\mathrm{SU}(2)_L \times \mathrm{U}(1)_R \times \mathrm{SU}(4)_C$ *intermediate breaking*, *Phys. Rev.* **D 49** (1994) 3704 [INSPIRE].

[62] M.K. Parida, *Heavy Particle Effects in Grand Unified Theories With Fine Structure Constant Matching*, *Phys. Lett.* **B 196** (1987) 163 [INSPIRE].

[63] M.K. Parida and B.D. Cajee, *High scale perturbative gauge coupling in R-parity conserving SUSY* SO(10) *with larger proton lifetime*, *Eur. Phys. J.* **C 44** (2005) 447 [hep-ph/0507030] [INSPIRE].

[64] S.K. Majee, M.K. Parida, A. Raychaudhuri and U. Sarkar, *Low intermediate scales for leptogenesis in SUSY* SO(10) *GUTs*, *Phys. Rev.* **D 75** (2007) 075003 [hep-ph/0701109] [INSPIRE].

[65] Particle Data Group collaboration, W.M. Yao et al., *Review of Particle Physics*, *J. Phys.* **G 33** (2006) 1 [INSPIRE].

[66] R.N. Mohapatra, *Mechanism for Understanding Small Neutrino Mass in Superstring Theories*, *Phys. Rev. Lett.* **56** (1986) 561 [INSPIRE].

[67] R.N. Mohapatra and J.W.F. Valle, *Neutrino Mass and Baryon Number Nonconservation in Superstring Models*, *Phys. Rev.* **D 34** (1986) 1642 [INSPIRE].

[68] D. Wyler and L. Wolfenstein, *Massless Neutrinos in Left-Right Symmetric Models*, *Nucl. Phys.* **B 218** (1983) 205 [INSPIRE].

[69] M.K. Parida and A. Raychaudhuri, *Inverse see-saw, leptogenesis, observable proton decay and* $\Delta_{\mathrm{R}}^{\pm\pm}$ *in SUSY* SO(10) *with heavy* W_R, *Phys. Rev.* **D 82** (2010) 093017 [arXiv:1007.5085] [INSPIRE].

[70] S.K. Majee, M.K. Parida and A. Raychaudhuri, *Neutrino mass and low-scale leptogenesis in a testable SUSY* SO(10) *model*, *Phys. Lett.* **B 668** (2008) 299 [arXiv:0807.3959] [INSPIRE].

[71] R. Lal Awasthi and M.K. Parida, *Inverse Seesaw Mechanism in Nonsupersymmetric* SO(10)*, Proton Lifetime, Nonunitarity Effects and a Low-mass Z' Boson*, *Phys. Rev.* **D 86** (2012) 093004 [arXiv:1112.1826] [INSPIRE].

[72] T. Fukuyama and T. Kikuchi, *Renormalization group equation of quark lepton mass matrices in the* SO(10) *model with two Higgs scalars*, *Mod. Phys. Lett.* **A 18** (2003) 719 [hep-ph/0206118] [INSPIRE].

[73] W. Grimus and L. Lavoura, *The seesaw mechanism at arbitrary order: Disentangling the small scale from the large scale*, *JHEP* **11** (2000) 042 [hep-ph/0008179] [INSPIRE].

[74] G.L. Fogli, E. Lisi, A. Marrone, A. Palazzo and A.M. Rotunno, *Evidence of* $\theta_{13} > 0$ *from global neutrino data analysis*, *Phys. Rev.* **D 84** (2011) 053007 [arXiv:1106.6028] [INSPIRE].

JHEP01(2015)045

[75] T. Schwetz, M. Tortola and J.W.F. Valle, *Global neutrino data and recent reactor fluxes: status of three-flavour oscillation parameters*, *New J. Phys.* **13** (2011) 063004 [arXiv:1103.0734] [INSPIRE].

[76] D.V. Forero, M. Tortola and J.W.F. Valle, *Global status of neutrino oscillation parameters after Neutrino-2012*, *Phys. Rev.* **D 86** (2012) 073012 [arXiv:1205.4018] [INSPIRE].

[77] A. Ilakovac and A. Pilaftsis, *Flavor violating charged lepton decays in seesaw-type models*, *Nucl. Phys.* **B 437** (1995) 491 [hep-ph/9403398] [INSPIRE].

[78] V. Cirigliano, A. Kurylov, M.J. Ramsey-Musolf and P. Vogel, *Lepton flavor violation without supersymmetry*, *Phys. Rev.* **D 70** (2004) 075007 [hep-ph/0404233] [INSPIRE].

[79] G.K. Leontaris, K. Tamvakis and J.D. Vergados, *Lepton and Family Number Violation From Exotic Scalars*, *Phys. Lett.* **B 162** (1985) 153 [INSPIRE].

[80] A. Ilakovac, A. Pilaftsis and L. Popov, *Charged lepton flavor violation in supersymmetric low-scale seesaw models*, *Phys. Rev.* **D 87** (2013) 053014 [arXiv:1212.5939] [INSPIRE].

[81] MEG collaboration, J. Adam et al., *New constraint on the existence of the $\mu^+ \to e^+\gamma$ decay*, *Phys. Rev. Lett.* **110** (2013) 201801 [arXiv:1303.0754] [INSPIRE].

[82] J. Barry and W. Rodejohann, *Lepton number and flavour violation in TeV-scale left-right symmetric theories with large left-right mixing*, *JHEP* **09** (2013) 153 [arXiv:1303.6324] [INSPIRE].

[83] M. Doi, T. Kotani and E. Takasugi, *Double beta Decay and Majorana Neutrino*, *Prog. Theor. Phys. Suppl.* **83** (1985) 1 [INSPIRE].

[84] J.D. Vergados, *The neutrinoless double beta decay from a modern perspective*, *Phys. Rept.* **361** (2002) 1 [hep-ph/0209347] [INSPIRE].

[85] K.S. Babu and R.N. Mohapatra, *Predictive neutrino spectrum in minimal* SO(10) *grand unification*, *Phys. Rev. Lett.* **70** (1993) 2845 [hep-ph/9209215] [INSPIRE].

[86] CMS collaboration, *Search for narrow resonances and quantum black holes in inclusive and b-tagged dijet mass spectra from pp collisions at $\sqrt{s} = 7$ TeV*, *JHEP* **01** (2013) 013 [arXiv:1210.2387] [INSPIRE].

[87] P. Nath and P. Fileviez Perez, *Proton stability in grand unified theories, in strings and in branes*, *Phys. Rept.* **441** (2007) 191 [hep-ph/0601023] [INSPIRE].

[88] M.K. Parida, *Radiative Seesaw in* SO(10) *with Dark Matter*, *Phys. Lett.* **B 704** (2011) 206 [arXiv:1106.4137] [INSPIRE].

[89] S. Bertolini, L. Di Luzio and M. Malinsky, *Light color octet scalars in the minimal* SO(10) *grand unification*, *Phys. Rev.* **D 87** (2013) 085020 [arXiv:1302.3401] [INSPIRE].

[90] SUPER-KAMIOKANDE collaboration, H. Nishino et al., *Search for Nucleon Decay into Charged Anti-lepton plus Meson in Super-Kamiokande I and II*, *Phys. Rev.* **D 85** (2012) 112001 [arXiv:1203.4030] [INSPIRE].

[91] S. Dimopoulos, S. Raby and G.L. Kane, *Experimental Predictions from Technicolor Theories*, *Nucl. Phys.* **B 182** (1981) 77 [INSPIRE].

[92] N.G. Deshpande and R.J. Johnson, *Experimental limit on* $SU(4)_C$ *gauge boson mass*, *Phys. Rev.* **D 27** (1983) 1193 [INSPIRE].

[93] M.K. Parida and B. Purkayastha, *New lower bound on* $SU(4)_C$ *gauge boson mass from CERN LEP measurements and $K_L \to \mu e$*, *Phys. Rev.* **D 53** (1996) 1706 [INSPIRE].

JHEP01(2015)045

[94] K. Arisaka et al., *Improved upper limit on the branching ratio $B(K_L^0 \to mu^{\pm}e^{\mp})$*, *Phys. Rev. Lett.* **70** (1993) 1049 [INSPIRE].

[95] K. Genezer, *The search for $n - \bar{n}$ oscillations at Super-Kamiokande-I*, In Proceedings of the *Workshop on (B-L) Violation*, Lawrence Berkeley Laboratory, september 20–22 2007, http://inpa.lbl.gov/BLNV/blnv.htm.

[96] W.-Y. Keung and G. Senjanović, *Majorana Neutrinos and the Production of the Right-handed Charged Gauge Boson*, *Phys. Rev. Lett.* **50** (1983) 1427 [INSPIRE].

[97] SUPER-KAMIOKANDE collaboration, J.L. Raaf, *Recent Nucleon Decay Results from Super-Kamiokande*, *Nucl. Phys. Proc. Suppl.* **229-232** (2012) 559 [INSPIRE].

[98] J.L. Hewett et al., *Fundamental Physics at the Intensity Frontier*, arXiv:1205.2671 [INSPIRE].

[99] K.S. Babu et al., *Working Group Report: Baryon Number Violation*, arXiv:1311.5285 [INSPIRE].

[100] S. Dimopoulos, S. Raby and G.L. Kane, *Experimental Predictions from Technicolor Theories*, *Nucl. Phys.* **B 182** (1981) 77 [INSPIRE].

[101] C.R. Das and M.K. Parida, *New formulas and predictions for running fermion masses at higher scales in SM, 2 HDM and MSSM*, *Eur. Phys. J.* **C 20** (2001) 121 [hep-ph/0010004] [INSPIRE].

[102] S. Antusch, J.P. Baumann and E. Fernandez-Martinez, *Non-Standard Neutrino Interactions with Matter from Physics Beyond the Standard Model*, *Nucl. Phys.* **B 810** (2009) 369 [arXiv:0807.1003] [INSPIRE].

[103] S. Antusch, M. Blennow, E. Fernandez-Martinez and J. Lopez-Pavon, *Probing non-unitary mixing and CP-violation at a Neutrino Factory*, *Phys. Rev.* **D 80** (2009) 033002 [arXiv:0903.3986] [INSPIRE].

[104] S. Antusch, C. Biggio, E. Fernandez-Martinez, M.B. Gavela and J. Lopez-Pavon, *Unitarity of the Leptonic Mixing Matrix*, *JHEP* **10** (2006) 084 [hep-ph/0607020] [INSPIRE].

[105] D.V. Forero, S. Morisi, M. Tortola and J.W.F. Valle, *Lepton flavor violation and non-unitary lepton mixing in low-scale type-I seesaw*, *JHEP* **09** (2011) 142 [arXiv:1107.6009] [INSPIRE].

[106] E. Fernandez-Martinez, M.B. Gavela, J. Lopez-Pavon and O. Yasuda, *CP-violation from non-unitary leptonic mixing*, *Phys. Lett.* **B 649** (2007) 427 [hep-ph/0703098] [INSPIRE].

[107] K. Kanaya, *Neutrino Mixing in the Minimal* SO(10) *Model*, *Prog. Theor. Phys.* **64** (1980) 2278 [INSPIRE].

[108] J. Kersten and A.Y. Smirnov, *Right-Handed Neutrinos at CERN LHC and the Mechanism of Neutrino Mass Generation*, *Phys. Rev.* **D 76** (2007) 073005 [arXiv:0705.3221] [INSPIRE].

[109] M. Malinsky, T. Ohlsson and H. Zhang, *Non-unitarity effects in a realistic low-scale seesaw model*, *Phys. Rev.* **D 79** (2009) 073009 [arXiv:0903.1961] [INSPIRE].

[110] G. Altarelli and D. Meloni, *CP violation in neutrino oscillations and new physics*, *Nucl. Phys.* **B 809** (2009) 158 [arXiv:0809.1041] [INSPIRE].

[111] F. del Aguila and J.A. Aguilar-Saavedra, *Electroweak scale seesaw and heavy Dirac neutrino signals at LHC*, *Phys. Lett.* **B 672** (2009) 158 [arXiv:0809.2096] [INSPIRE].

JHEP01(2015)045

[112] F. del Aguila, J.A. Aguilar-Saavedra and J. de Blas, *Trilepton signals: the golden channel for seesaw searches at LHC*, *Acta Phys. Polon.* **B 40** (2009) 2901 [arXiv:0910.2720] [INSPIRE].

[113] A. van der Schaaf, *Muon physics at a neutrino factory*, *J. Phys.* **G 29** (2003) 2755 [INSPIRE].

[114] B.P. Nayak and M.K. Parida, *New mechanism for Type-II seesaw dominance in* SO(10) *with low-mass Z-prime, RH neutrinos and verifiable LFV, LNV and proton decay*, arXiv:1312.3185 [INSPIRE].

[115] E.C. F.S. Fortes, K.S. Babu and R.N. Mohapatra, *Flavor Physics Constraints on TeV Scale Color Sextet Scalars*, arXiv:1311.4101 [INSPIRE].

[116] E. Witten, *Neutrino Masses in the Minimal* $O(10)$ *Theory*, *Phys. Lett.* **B 91** (1980) 81 [INSPIRE].

[117] C. Arbeláez Rodríguez, H. Kolešová and M. Malinský, *Witten's mechanism in the flipped* SU(5) *unification*, *Phys. Rev.* **D 89** (2014) 055003 [arXiv:1309.6743] [INSPIRE].

[118] S.M. Barr, *A New Symmetry Breaking Pattern for* SO(10) *and Proton Decay*, *Phys. Lett.* **B 112** (1982) 219 [INSPIRE].

[119] S.M. Barr, *Some Comments on Flipped* SU(5) × U(1) *and Flipped Unification in General*, *Phys. Rev.* **D 40** (1989) 2457 [INSPIRE].

[120] C.R. Das, C.D. Froggatt, L.V. Laperashvili and H.B. Nielsen, *Flipped* SU(5)*, see-saw scale physics and degenerate vacua*, *Mod. Phys. Lett.* **A 21** (2006) 1151 [hep-ph/0507182] [INSPIRE].

[121] I. Dorsner and P. Fileviez Perez, *Distinguishing between* SU(5) *and flipped* SU(5), *Phys. Lett.* **B 605** (2005) 391 [hep-ph/0409095] [INSPIRE].

[122] P.S.B. Dev and R.N. Mohapatra, *TeV Scale Inverse Seesaw in* SO(10) *and Leptonic Non-Unitarity Effects*, *Phys. Rev.* **D 81** (2010) 013001 [arXiv:0910.3924] [INSPIRE].

[123] C. Arbeláez, M. Hirsch, M. Malinský and J.C. Romão, *LHC-scale left-right symmetry and unification*, *Phys. Rev.* **D 89** (2014) 035002 [arXiv:1311.3228] [INSPIRE].

JHEP01(2015)045